UNIVERSITY OF MOLISE

DEPARTMENT OF BIOSCIENCES AND TERRITORY

PhD Programme in
BIOLOGICAL AND ENVIRONMENTAL SCIENCES AND TECHNOLOGIES
XXVIII CICLE

DORIANA DESIDERIO

Biochemical approaches to study protein–ligand interaction for pharmacological applications

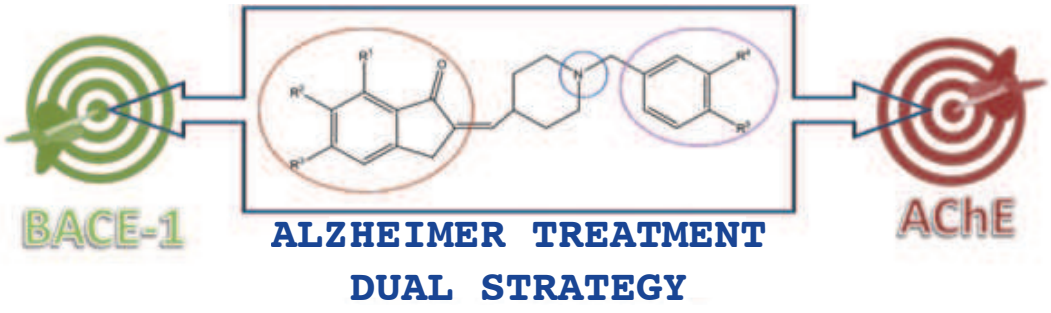

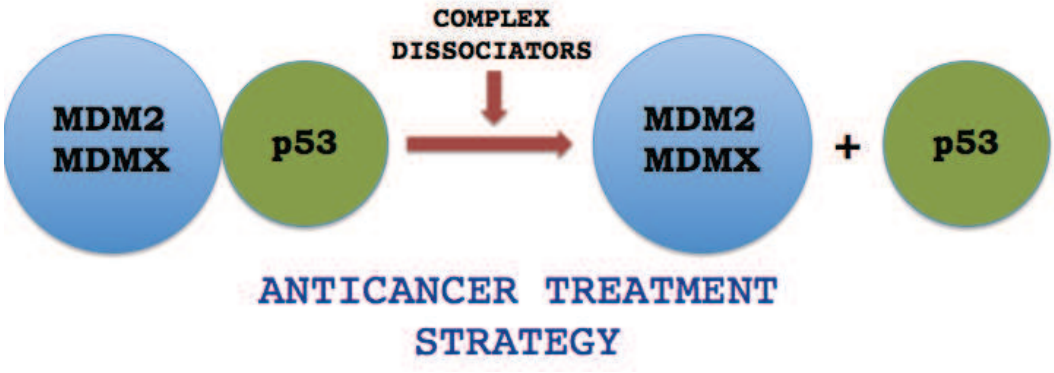

Academic Year 2014/2015

UNIVERSITY OF MOLISE

DEPARTMENT OF BIOSCIENCES AND TERRITORY

PhD Programme in

BIOLOGICAL AND ENVIRONMENTAL SCIENCES AND TECHNOLOGIES

XXVIII CICLE – S.S.D. BIO/10

Biochemical approaches to study protein–ligand interaction for pharmacological applications

Tutor
Chiar.mo Prof.
Gennaro RAIMO

Coordinator
Chiar.mo Prof.
Claudio CAPRARI

Candidate
Doriana DESIDERIO
Matr. n.°149512

Academic Year 2014/2015

A te

Abstract

This work is focused on the application of simple biochemical techniques to study protein-ligand interaction involved in some diseases of frequent incidence, such as Alzheimer's disease (AD) and cancer.

The current therapies for AD, still symptomatic and palliative, from one side act to inhibit AChE, in order to restore the natural level of ACh, and, from the other side act as inhibitors of β-secretase 1 (BACE-1), useful to prevent the Aβ aggregation. Under this regard, efforts have been recently devoted to the development of dual inhibitors of AChE and BACE-1.

In this frame, donepezil-like compounds were synthesised, in order to identify novel effective drugs for the treatment of AD. For all these new synthesized analogues, more rigid and diversely substituted compared to donepezil structure, the inhibitor activity on AChE, the selectivity vs BuChE, the side-activity on BACE-1 and the effect on SHSY-5Y neuroblastoma cell viability were tested. Two potential new lead compounds for a dual therapeutic strategy against Alzheimer disease were envisaged.

Activation of p53 tumor suppressor by antagonizing its negative regulators MDM2/X has been considered an attractive strategy for cancer therapy. Great effort has been given in the development of drugs able to dissociate the p53·MDM2/X complex. Under this regard, a simple and rapid technique to study the p53–MDM2/X interaction has been developed. This method is based on the different mobility between the interacting domains of the oncosuppressor p53 and its protein ligands MDM2/X on polyacrylamide gels under native conditions. While the two proteins MDM2/X alone were able to enter the gel, the formation of a

binary complex between p53 and MDM2/X prevented the gel entry. The novel technique is reliable for determining the different affinity elicited by MDM2 or MDMX toward p53, and for analyzing the dissociation power exerted by small molecules on the complex taking advantage of the appearance of migrating MDM2 or MDMX, when inhibitors are added to the complex mixture. Despite the fact that some other different methods have been employed to study this kind of interaction, including NMR technology, surface plasmon resonance or fluorescence polarization, the relevance of the method here described resides in the fact that it is much more simple and it does not require any tagging/derivatization procedure of the protein fragments employed. This simple and rapid technique can be useful to easily discriminate, among a library of compounds endowed with a potential pharmacological activity against cancer development, the molecules with the highest dissociative potency, preventing the use of expensive and more sophisticated technologies.

General introduction

Proteins play pivotal and essential roles in cellular activity. For this reason, protein–ligand interactions are fundamental for almost all processes occurring in living organisms. Ligand-mediated signal transmission through molecular complementary is essential to all life processes; these chemical interactions comprises biological recognition at molecular level. The evolution of the protein function is dependent in part on the development of highly specific sites designed to bind ligand molecules with affinities tuned to the needs of the cell. Ligand binding capacity is important for the regulation of biological functions. Regulation of cellular processes via cooperative protein–ligand interactions occurs through molecular mechanisms involving protein conformational transition among low– and high–affinity states. Ligand binding interactions changes the protein state and protein function.

Because protein-ligand interactions play a key role in cellular metabolism, detailed knowledge of such interactions, either at a microscopic and macroscopic level, is also required. Important systems, which are now being studied at a molecular level, include ligand binding to structural proteins, protein-DNA binding, protein-saccharide, protein-protein, and protein-peptide interactions.

The term “ligand” in biological systems can have many different meanings. In its broadest sense, it is usually used to intend any molecule which interacts with a given molecule (in this case a protein). The term “ligand” thus includes other macromolecules (peptides/proteins/nucleic acids/lipids/carbohydrates or mixed molecular species thereof) as well as “small” molecular mass molecules (arbitrarily < 1-2 kDa). Ligands therefore comprise a very large and structurally diverse group of

molecules which, unsurprisingly also display a wide variety of physic-chemical characteristics. This makes it difficult to understand, delineate, and draw generalized conclusions concerning their biophysical properties.

When possible, the knowledge of the structure/conformation at the atomic level of the protein and the ligand in the unbound form represents a prerequisite for protein-ligand interaction studies.

For example, the structures of protein–ligand complexes at atomic resolution make possible the design of small-molecule drugs for the treatment of diseases.

The study of interactions between proteins and cellular molecules is fundamental to the understanding of biological systems. Drastically increased interest in this problem among investigators working in different fields of biological science needs to be supported by knowledge of biophysical tools and approaches dealing with protein interactions.

Protein-ligand interaction can be studied with a large variety of biophysical techniques such as the surface plasmon resonance (SPR), the isothermal titration calorimetry (ITC), the mass spectrometry (MS), the microscale thermophoresis (MST), the nuclear magnetic resonance (NMR), and so on.

Under this regard, the research work dealing with this PhD thesis is focused on the adaptation of common and simple biochemical techniques to the study the protein-ligand interactions involved in some frequent incidence diseases, such as Alzheimer's disease and cancer. For both topics, the research approach was multidisciplinary, considering the partnership with other groups experienced in pharmacology, bio-informatics, organic chemistry, molecular biology, and of course, in biochemistry.

Chapter I

Identification of Donepezil analogues as dual inhibitors for the Alzheimer's disease treatment

I.1 State of art on the Alzheimer's disease

Alzheimer's disease (AD), named after the doctor who first described it in 1907 (Alois Alzheimer), is a neurodegenerative disorder of the Central Nervous System (CNS). It is characterised by progressive deterioration of memory and higher cortical functions that ultimately result in total degradation of intellectual and mental activities.

AD is the most common form of dementia. It is one of the major health problems in the economically developed countries along with cardiovascular disorders and cancer. In fact, it is estimated that currently about 36 million people in the world suffering from AD and it is expected that they will be 66 million in 2030 [Wold Alzheimer Report, 2011]. Its prevalence increases with age, from 10% at 65 years to nearly 50% at 85 years [Bachurin, 2003; Colombres et al., 2004].

At the macroscopic level, in Alzheimer's disease a variable degree of cortical atrophy, characterized by enlargement of the parietal grooves, more pronounced in the frontal lobes, temporal and parietal, can be observed. This atrophy is compensated by an enlargement of the ventricular cavities, secondary event to the loss of parenchyma. In particular, in the advanced stages of the disease, the structures of the medial temporal lobe, including the hippocampus, entorhinal cortex and amygdala, result severely atrophied, given their involvement starting from the earliest stages of the disease.

Alzheimer's disease also presents even microscopic changes, known as extracellular senile plaques and intracellular neurofibrillary tangles, which form the basis of histological diagnosis. When the progression of the disease occurs, a severe neuronal loss is accompanied by gliosis.

The neuropathological characteristics keys of AD are senile plaques (SP), which are associated with beta-amyloid peptide, neurofibrillary tangles (NFT), and the loss of neurons in the hippocampus and nucleus basalis of Meynart [Selkoe, 1991; Goedert et al., 1996; Morrison et al., 1998]. Neurotransmitter specificity of AD is characterised by a pronounced degradation of cholinergic system and by disturbances of functions in other neurotransmitter systems, such as glutamatergic and serotoninergic systems [Dringenberg, 2000; Buccafusco & Terry, 2000].

According to the ‘‘cholinergic hypothesis’’, impairment in the cholinergic function is of critical importance in AD especially for the brain areas dealing with learning, memory, behaviour and emotional responses that include the neocortex and the hippocampus. Brain atrophy is the most obvious clinical finding in AD in which the levels of acetylcholine (ACh), a neurotransmitter responsible for the conduction of electrical impulses from one nerve cell to another nerve cell, are decreased due to its rapid hydrolysis by acetylcholinesterase (AChE) enzyme [Ladner & Lee, 1998].

According to ‘‘amyloid hypothesis’’, AChE produces secondary non-cholinergic functions that include promotion beta-amyloid peptide (Ab) deposition in the senile plaques/neurofibrillary tangles in the brain of afflicted individuals [Castro & Martinez, 2001; Selkoe, 2002; Bartolini et al., 2003; Rees et al., 2003]. The deposition of Ab has been considered to play an important role in the initiation, as well as in the progression, of AD [Rees et al., 2003]. In addition, in the amyloid hypothesis the formation and the aggregation of the β-amyloid peptide (Aβ) [Eikelenboom et al., 2006] has been associated to the hydrolysis of the

Amyloid Precursor Protein (APP) by β-secretase 1 (BACE-1) [Vassar et al., 2004].

Butirrylcholinesterase (BuChE) is an enzyme closely related to AChE, working as a co-regulator of cholinergic neurotransmission by hydrolysing ACh [Mesulam et al., 2002]. The studies have shown an increased BuChE activity (40–90%) in the most affected areas of the brain, such as the temporal cortex and the hippocampus, during the development of AD. An increased BuChE activity plays also an important role in Ab-aggregation during the early stages of senile plaque formation [Geula & Darvesh, 2004]. Thus, AChE and BuChE inhibition have been documented as critical targets for the effective management of AD by an increase in the availability of ACh in the brain regions and decrease in the Ab deposition [De Ferrari et al., 2001]. However, BuChE is mainly localized in the peripheral tissues, including plasma, but accounting for a very small amount in the brain region. Therefore, the potential advantage of selective inhibition of AChE over BChE may include lower degree of associated side effects due to peripheral inhibition of cholinesterase enzyme [Anand & Singh, 2012b].

Nowadays, no cure for Alzheimer's is so far available. Researchers are still trying to fully understand how the disease leads to memory loss and problems regarding thinking and behaviour, hoping to prevent or stop the disease.

Some therapies ease the symptoms and help people to feel better for longer. Because the disease's effects change over time, people often need personalised treatments which changes during time, when different related to AD problems emerge.

The current therapies for AD, still symptomatic and palliative, works, from one side, for the inhibition of AChE to restore the natural level of ACh [Bolognesi et al., 2002; Zhang & casida, 2005], and, from the other side, on the inhibition of Aβ aggregation [Eikelenboom et al., 2006; Mancini et al., 2007]. Under this regard, efforts have been recently devoted to the development of dual inhibitors of AChE and BACE-1 [Zhu et al., 2009; Viayna et al., 2013; Ortega et al., 2011; Rampa et al., 2015; Nguyen et al., 2015].

The approved drugs against AD causes or effects can be divided in two classes:

- drugs for Alzheimer's disease;
- drugs for other induced disorders.

Acetylcholinesterase inhibitors are commonly used to treat mild to moderate stage of Alzheimer's disease. These drugs increase the cholinergic transmission, delaying the degradation of acetylcholine. They maintain the availability of acetylcholine in the brain and can make up, but not stop, the cell destruction caused by the disease.

The AChE drugs approved by the *U.S. Food and Drug Administration* (FDA) are:

- Tacrine (in Italy is not available)
- Rivastigmine
- Galantamine
- Donepezil

Tacrine was the first centrally acting cholinesterase inhibitor approved for the treatment of Alzheimer's disease in 1993 by the U.S. FDA, and was marketed under the trade name **Cognex®**.

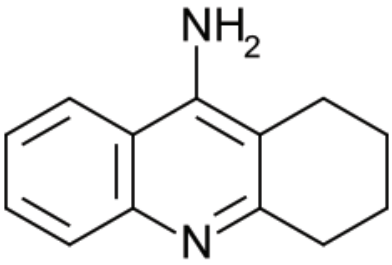

Figure I.1. The structure of Tacrine

Despite this drug is able to lead an improvement of cognitive functions, its side effects, particularly on the liver, doesn't make it a first choice remedy.

The rivastigmine, better known as **Exelon**®, is also used for Alzheimer's disease, and it was observed that acts mostly on the brain areas such as hippocampus and cortex.

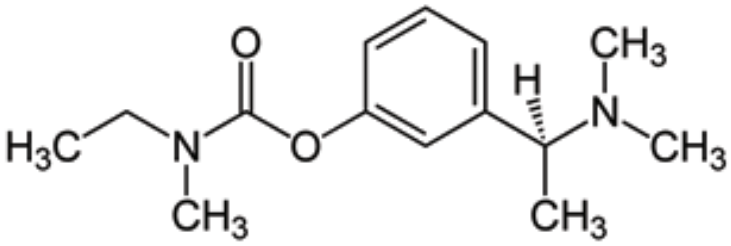

Figure I.2. The structure of Rivastigmine

One of the newer cholinesterase inhibitors is galantamine, approved by the FDA in 2001. This molecule is known by the trade name **Reminyl**®, and it is a natural alkaloid found in Galanthus nivalis, a plant belonging to the family Amaryllidacea. Since its discovery, galantamine has been used for the treatment of myasthenia gravis (muscle weakness) and other neuromuscular diseases. For its ability to cross the blood-brain barrier (at the level of the central nervous system) and to selectively

inhibit AChE, its use in the treatment of Alzheimer's disease has been suggested. It is a long lasting drug with activity on the central nervous system, devoid of toxicity at the hepatic level and with moderate side effects, similar to those of the other cholinesterase inhibitors. The administration of galantamine has prompted an increase of memory performance in treated subjects, leading to a reduction of the cognitive damage.

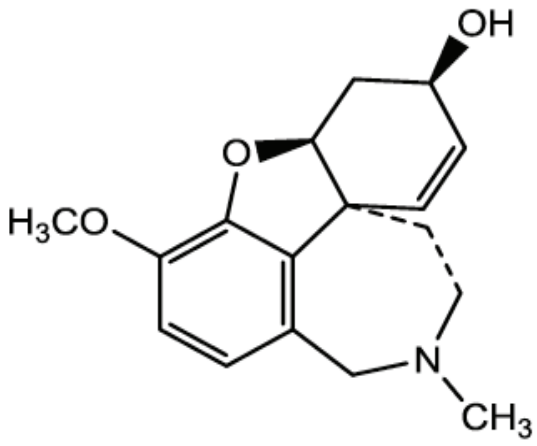

Figure I.3. The structure of Galantamine

Among the several drugs approved by the FDA-USA for the treatment of AD, the most recently one is donepezil, better known by the trade name **Aricept**®. Donepezil has a half-life of about 70 hours, that makes possible a only one daily administration. It acts in the early stage of disease, when it is still considered mild or moderate. At this stage the cognitive symptoms are still mild and the everyday life of the patient is not compromised. Furthermore, Donepezil has shown an excellent tolerability without hepatotoxicity and is considered the most effective inhibitor of the AChE currently available on the market [Sugimoto et al.,

2000; Van der Zee et al., 2001]. Very recently donepezil has been proposed as soft inhibitor of β-secretase 1.

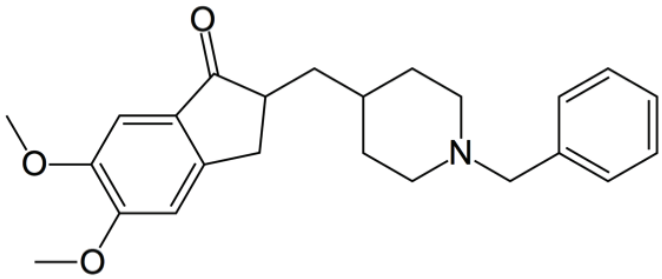

Figure I.4. The structure of Donepezil

The profile of the adverse effects of various acetylcholinesterase inhibitors is similar, and include gastrointestinal effects such as nausea, vomiting, weight loss and neurological effects including insomnia, headaches, dizziness, sweating. The choice of one or the other drug depends on the doctor and varies from individual to individual. The disadvantage of using these drugs is that their efficacy is related to the integrity of the nervous structures, which in the Alzheimer's patient continue to degenerate, reducing the acetylcholinesterase inhibitors effect. Furthermore, another disadvantage is the lack of selectivity towards specific receptors. In particular, numerous scientific studies have shown that stimulation of muscarinic receptors of type M1, but not M2, is able to lead to a reduction in the levels of β–amyloid.

I.2 The aim

The aim of the present work is to design, on the basis of molecular docking strategy, and to synthesize, through eco-friendly synthetic procedures, donepezil-like compounds as potential AChE and BACE-1 inhibitors, in order to identify novel effective drugs for the treatment of AD.

For all these compounds the evaluation of their inhibitory effect on the catalytic activity of cholinesterases was followed by spectrophotometric method, whereas that on β-secretase activity was monitored by spectrofluorimetric method. In addition, the effect on cell viability and the possible cytotoxicity on neurons cell line, has also been investigated.

I.3 Experimental

I.3.a *Materials*

All donepezil-like compounds have been synthesized and given by the research group of Professor Antonio Procopio of Department of Health Sciences, University of the Studies of Magna Graecia. All the compounds were identified by HR-MS and characterized by ^{1}H-NMR and ^{13}C-NMR.

AChE from *Electrophorus electricus* (eeAChE), and from human erythrocytes (hAChE), BuChE from horse serum, acetylthiocholine, butyrylthiocholine, 5, 5'-dithiobis-2-nitrobenzoic acid (DTNB), Donepezil, the fluorescent peptide substrate containing the Lys-Met/Asn-Leu mutations cleavage site of the amyloid precursor protein (APP) β-secretase, the MTT (3-(4,5-dimethylthiazol-2-yl)-2,5-diphenyltetrazolium bromide) and the Trypan blue dye (2,7-Naphthalenedisulfonic acid, 3,3'-((3,3'-dimethyl(1,1'-biphenyl)-4,4'-diyl)bis(azo))bis(5-amino-4-hydroxy-), tetrasodium salt) were purchased from Sigma-Aldrich.

Mouse BACE-1 (recombinant) and BACE-1 Inhibitor I were from Life Technology, and BACE-1 inhibitor IV solution (10 mM in DMSO) was from Calbiochem.

Stock solutions of the synthesized compounds were prepared in DMSO at 100 mM final concentration.

I.3.b *Enzymatic assays*

Cholinesterase activity was assayed by the Elmann method [Ellman et al., 1961] using acetylthiocholine or butyrylthiocoline as substrate for AChE or BuChE, respectively. The reduction of

dithiobisnitrobenzoate by the thiocholine, produced by the enzymatic hydrolysis of thiolated substrates, was followed colorimetrically (412 nm) at room temperature (22-27°C). The reaction mixture (500 μL) contained 330 μM DTNB and the appropriate amount of substrate, in 0.1 M sodium phosphate buffer, pH 7.1. The reaction was started by the addition of 100 mU/mL or 200 mU/mL of AChE or BuChE, respectively, and the initial rate of the reaction was derived from the linear portion of the kinetics.

The reversibility of the inhibitory activity exerted by all synthesised compounds was assessed using a dilution method described previously [Sohn et al., 2003; Lavecchia et al., 2012]. Briefly, the enzyme was pre-incubated for 20 min with the inhibitors or with DMSO, as a vehicle control; after a 100-fold dilution of the reaction mixture, the residual enzyme activity was measured as reported above.

The concentration of inhibitor required to reduce the enzymatic activity to 50% (IC_{50}) was derived from semi-logarithmic plots in which the residual cholinesterase activity was determined at different concentration of inhibitor, using a thiolated substrate concentration of 500 μM. Linear curve fits were obtained with the least-squares method, and the significance of the correlation was estimated from the squared correlation coefficient r^2, which was always higher than 0.95.

The kinetic parameters of the enzymatic reaction, K_m and V_{max}, were derived from the determination of the enzyme activity at 6 different acetylthiocholine or butyrylthiocholine concentration (80–500 μM), chosen in order to give the similar weight in the regression. The data were either interpolated in the Michaelis-Menten equation or treated with the Lineweaver-Burk equation giving similar results.

The inhibition constant K_i was derived by measuring the kinetic parameters in the presence of different inhibitor concentration, 0.2 – 30 μM for AChE or 3 – 100 μM for BuChE. The values of K_i were derived from the equation $K_m' = K_m (1 + [I]/K_i)$, in case of competitive inhibition or $V_{max}' = V_{max} / (1 + [I]/K_i)$, in case of non-competitive inhibition, or with both in the case of mixed inhibition. In these equations K_m' and V_{max}' represent the values of K_m and V_{max} measured at the [I] concentration of inhibitor. Values of IC_{50} and K_i reported were the mean of at least 4 different determinations.

BACE-1 activity was assayed by a fluorimetric method [Mancini et al., 2007] using the Enspire™ Multimode Plate Reader (Perkin-Elmer) in the kinetic Fluorescence method. The assay was performed in black polystyrene 96-well microtiter plates. The reaction mixtures contained 2.1 ng/μL mouse BACE-1 in 50 mM ammonium acetate buffer, pH 4.5, supplemented with 1 mM triton X-100, and the appropriate amount of the inhibitor. The mixture was incubated for 10 min at room temperature (22-25°C), the reaction started by adding 100 nM final concentration of the fluorescent peptide substrate, and the increase in fluorescence was followed kinetically. The enzymatic cleavage of the peptide led to the appearance of a fluorescence signal using excitation and emission wavelength of 320 and 420 nm, respectively. The rate was derived from the linear portion of the kinetics, usually in the first 30 min of the reaction. The known Inhibitors I (IC_{50}, 240 nM) [Lavecchia et al., 2012], and IV (IC_{50}, 15 nM) [Stachel et al., 2004], were used as positive controls.

I.3.c *Proliferation and viability assays*

The effect of the synthesized compounds on proliferation and viability was assessed in SH-SY5Y neuroblastoma cells. Cells were grown in Roswell Park Memorial Institute medium (RPMI) supplemented with 2 mM L-glutamine, 100 UI/mL penicillin, 100 µg/mL streptomycin and 10% (v/v) fetal bovine serum. Cells were maintained in culture dishes Petri 100 mm, at 37 °C in a saturated humidity atmosphere containing 95% air and 5% CO_2. Cells were seeded at an initial density of 10^4 cells/cm^2 in culture dishes. At a confluence of 80%, cells were detached by trypsin treatment, suspended in fresh medium without FBS and transferred to multiwell (6, 12 or 96 wells) according to the experimental requirements. After 24h from seeding, cells were incubeted with different synthesized compounds for 24-48 hours using 0.1% (v/v) DMSO as vehicle.

The effect of synthesized compounds on cell proliferation was evaluated as mitochondrial activity using the MTT (3-(4,5-dimethylthiazol-2-yl)-2,5-diphenyltetrazolium bromide) assay [Mossman, 1983]. Briefly, after the treatment, the medium was removed and cells were incubated with 100 µL MTT solution (0.5 mg/mL) for 1 h. After that, the solution was removed, the formed formazan was solubilized in 100 µL of 0.1 N HCl in 90 % (v/v) 2-propanol and the absorbance measured at 570 nm using a microplate reader (BioRad).

Vice versa, cell viability was evaluated using Trypan blue exclusion method [Strober, 2001] based on the principle that living cells possess intact cell membranes avoid the entrance of the dye, whereas dead cells does, rendering blue their cytosol. After the incubation with the compounds, the medium was removed to eliminate cells in suspension,

and the adherent cells were detached through trypsin treatment. The cell suspension was then centrifuged at 1200 rpm for 5 minutes and the cell pellet was resuspended with 0.4% (p/v) of Trypan blue.

I.4 Results and Discussion

I.4.a *Synthesis of Donepezil analogues*

In the last decade, it has spent a lot of effort in the synthesis of pharmacologically active molecules through eco-friendly synthetic procedures in agreement with the known principles of green chemistry [Procopio et al., 2014; Nardi et al., 2011; Cravotto et al., 2011; Oliviero et al., 2014]. Thus, inspired by this philosophy, it was designed the general synthetic pathway for the novel donepezil derivatives depicted in Fig. I.5.

The X-ray crystallographic studies for a large number of AChE–ligand complexes show as two main binding sites the catalytic binding site (CAS), comprising the Ser-His-Glu catalytic triad, and the secondary/peripheral anionic binding site (PAS), connected by a deep, hydrophobic gorge [http://www.rcsb.org/pdb/home/home.do]. Donepezil, (*RS*)-2-[(1-benzyl-4-piperidyl) methyl]-5,6-dimethoxy-2,3-dihydroinden-1-one, known also as E2020, can interact with both the sites: the *N*-benzyl piperidine residue binds to the CAS of AChE, whereas the hydrophobic aromatic part (5,6-dimethoxyindan-1-one) binds to the PAS [Koellner et al., 2000, Saxena et al., 2003].

Based on these observations, a series of indanone and piperidine derivatives bearing electron-donating groups on the different positions of the respective aromatic rings, which would lead to the synthesis of various derivatives of donepezil by aldol condensation, were designed (Fig. I.6).

The general structure of the designed compounds (Fig. I.6) maintains the *N*-benzyl piperidine and indanone moieties of the donepezil structure identified as important interactions binding sites with AChE but the stereocenter between them was eliminated, because there are no

evidences about its role in donepezil binding action. In all the synthesized compounds an unsaturation was located between the indanone and benzilpiperideine moieties, leading to a more rigid structure. It has been recently proposed that donepezil analogues with a double bond on the indanone moiety can act as BACE-1 inhibitors due to their structural rigidity. Two series of Donepezil like compounds were devoleped and synthesized: a methoxyl 10-components series, characterized by the presence of methoxyl groups in different structural positions (GP9, GP10, GP11, GP12, GP13, GP15, GP16, GP17, GP18, GP19).

On the basis of molecular docking analysis these modifications should ensure a better interaction with the cholinesterase and BACE-1 catalytic sites.

Finally, with the aim at improving compound solubilisation, a different phenolic 4-components series was synthesized (DEMG3, DEMG5, DEMG6, DEMG7), in order to study if a stronger H-donor group can influence the binding on the CAS. According to the docking studies performed on these molecules, the amino substituent reached the enzyme active site, while the indanone substituents were exposed to the solvent [Rampa et al., 2015]. For this reason it was decided to test the new donepezil analogues also against BACE-1 activity.

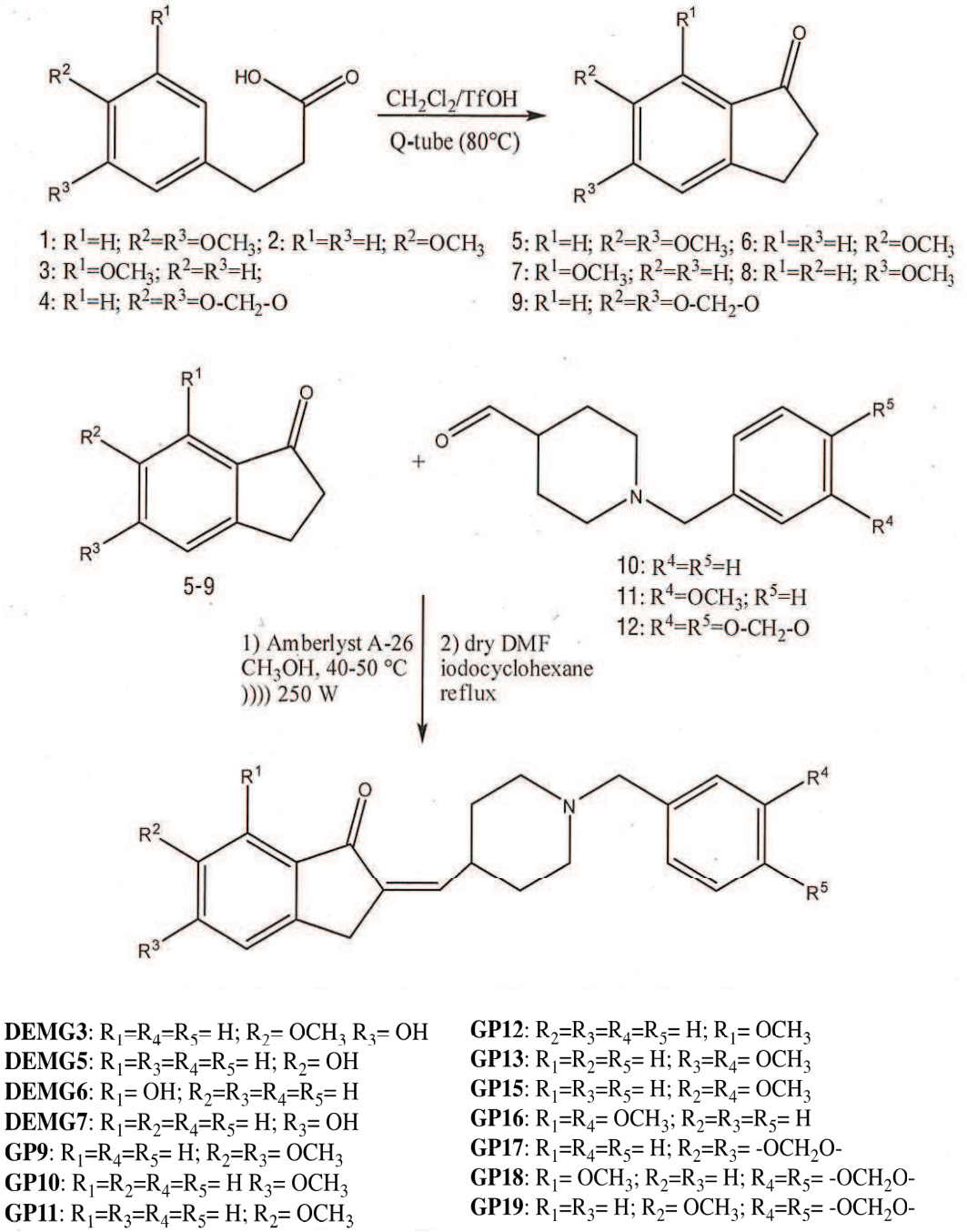

DEMG3: R_1=R_4=R_5= H; R_2= OCH_3 R_3= OH
DEMG5: R_1=R_3=R_4=R_5= H; R_2= OH
DEMG6: R_1= OH; R_2=R_3=R_4=R_5= H
DEMG7: R_1=R_2=R_4=R_5= H; R_3= OH
GP9: R_1=R_4=R_5= H; R_2=R_3= OCH_3
GP10: R_1=R_2=R_4=R_5= H R_3= OCH_3
GP11: R_1=R_3=R_4=R_5= H; R_2= OCH_3
GP12: R_2=R_3=R_4=R_5= H; R_1= OCH_3
GP13: R_1=R_2=R_5= H; R_3=R_4= OCH_3
GP15: R_1=R_3=R_5= H; R_2=R_4= OCH_3
GP16: R_1=R_4= OCH_3; R_2=R_3=R_5= H
GP17: R_1=R_4=R_5= H; R_2=R_3= -OCH_2O-
GP18: R_1= OCH_3; R_2=R_3= H; R_4=R_5= -OCH_2O-
GP19: R_1=R_3= H; R_2= OCH_3; R_4=R_5= -OCH_2O-

Figure I.5. Synthetic pathway for the total synthesis of Donepezil analogues

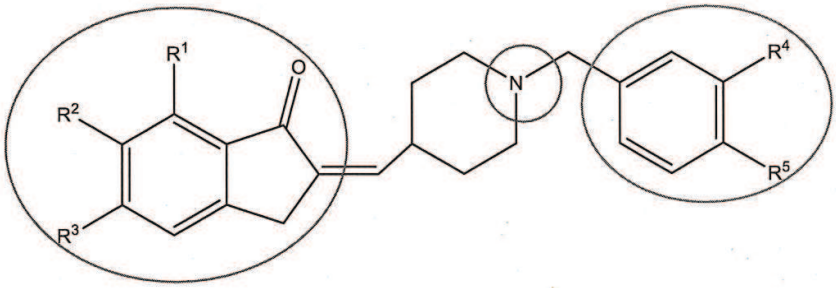

Figure I.6. Chemical structure of designed Donepezil analogues

I.4.b *Effect of the synthesized compounds on the kinetic parameters of cholinesterases*

To test the inhibition power of synthesized compounds, the *Electrophorus electricus* and *human* acetylcholinesterase (eeAChE, hAChE respectively) activity was measured in the absence or in the presence of 1 μM of each compound; when butyrylcholinesterase for horse serum (BuChE) activity was tested, the 2 μM concentration of each compound was used.

The effect of the inhibitors on cholinesterases activity was compared to that exhibited by Donepezil (Fig. I.7). Among the tested compounds, **GP10**, **GP9**, **GP11**, and **DEMG6** (see Fig. I.5 for their molecular structures) exhibited the highest inhibition on hAChE activity, with an estimated IC_{50} below 1 μM, therefore approaching that of Donepezil (Panel A, Fig. I.7).

In the case of eeAChE, in addition to the above mentioned compounds, also **GP12** exhibited one of the greatest inhibitory activity (Panel B, Fig. I.7); although the inhibitory effect was lower than that exhibited by donepezil, their IC_{50} still remain below 1 μM.

Concerning BuChE activity, the inhibition power of all the synthesized compounds was always lower (Panel C, Fig. I.7), being the IC_{50} values higher than 2 μM.

As demonstrated by the dilution method (see section 3.I.2), the inhibitory effect observed was reversible for all cholinesterases tested because the activity was recovered after a 100-fold dilution of every added compound; the only exception was observed for Donepezil effect on both eeAChE and hAChE, since 10 nM final concentration still inhibiting this enzymatic activity (not shown).

Therefore, in order to determine the IC_{50} of the synthesized compounds on cholinesterases, the residual enzymatic activity was assessed following the addition of different amounts of the inhibitors to the reaction mixture. In Panels A (methoxylic derivatives) and B (hydroxylic derivatives) of Fig. I.8 the effect on eeAChE activity was shown; the data were then treated in a semilogarithmic plot (Panel C and D, Fig. I.8), in order to extrapolate the values of the IC_{50}.

The results obtained from the experiments on eeAChE were reported in Table I.1. Those obtained from the similar experiments carried out on hAChE and BuChE (not shown), were instead reported in Table I.2.

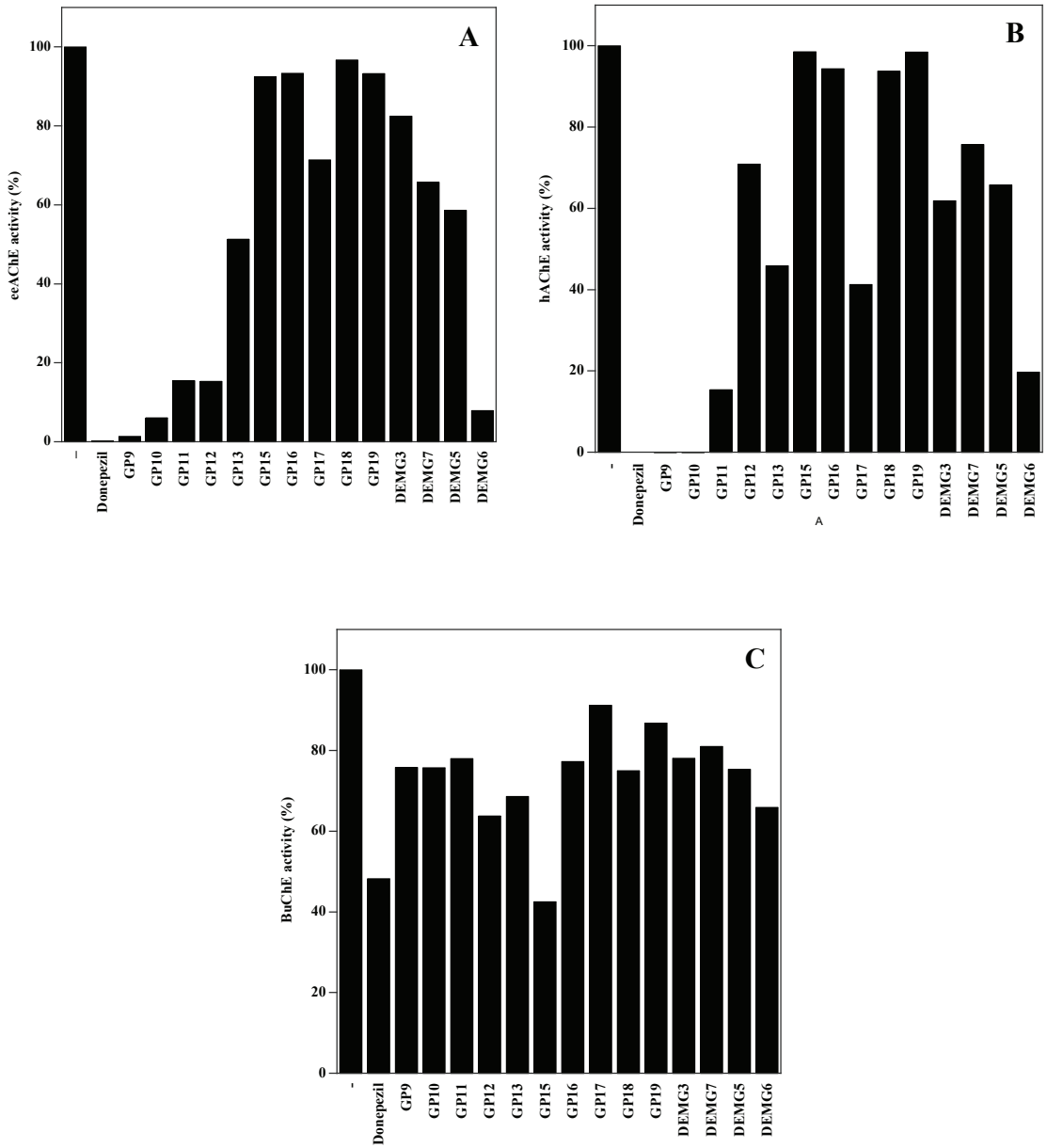

Figure I.7. Inhibition of the cholinesterase activity exerted by synthesized compounds.

The cholinesterase activity was determined in the absence or in the presence of the indicated compounds. Panel A: effect on eeAChE activity due by compounds added to 1 μM final concentration; panel B: effect on hAChE activity due by compounds added to 1 μM final concentration; panel C: effect on BuChE activity due by compounds added to 2 μM final concentration. The data represent the average of at least three different determinations. Further experimental details are given in section I.3.b.

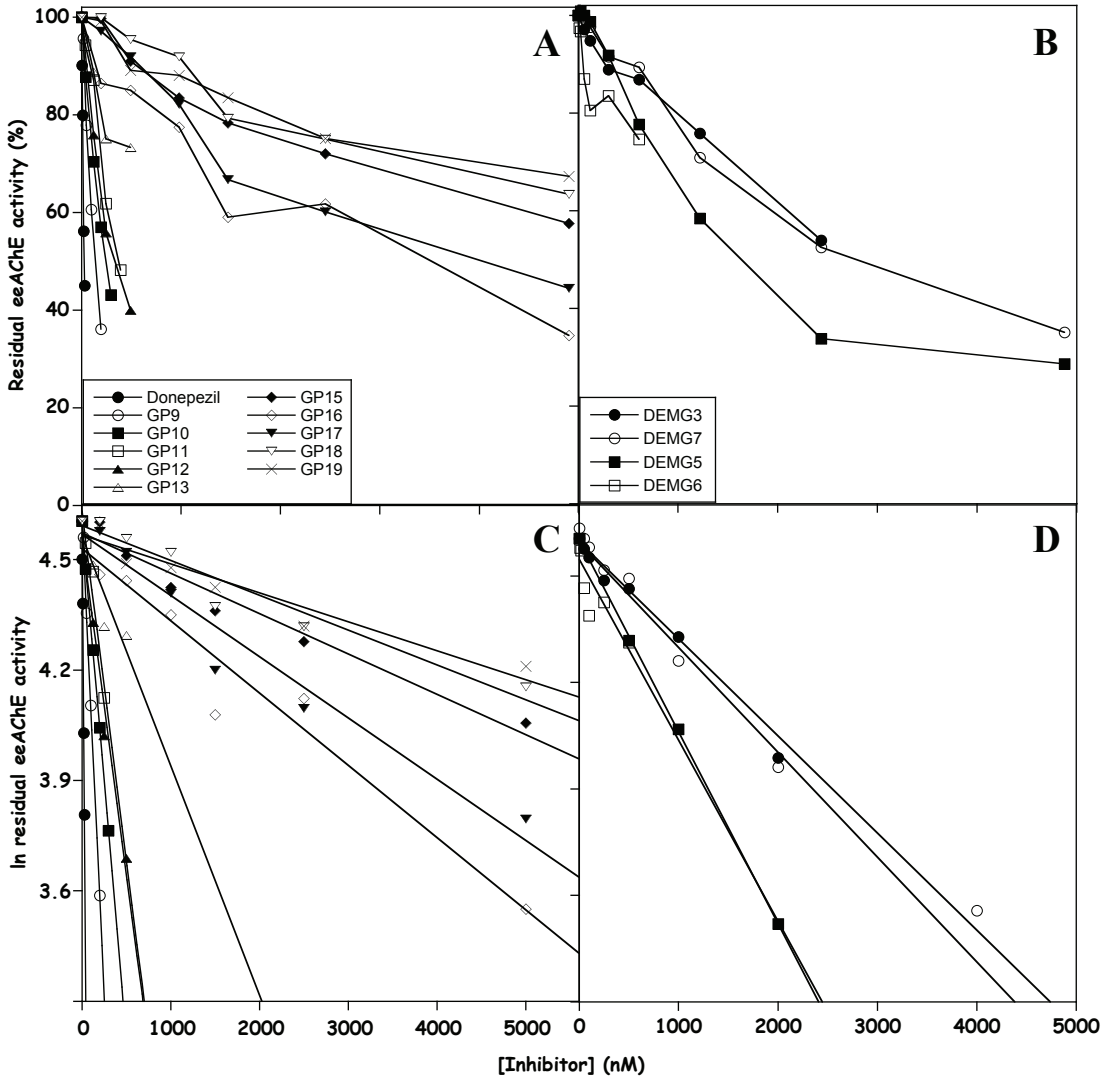

Figure I.8. Determination of the IC_{50} of the synthesized compounds.

Table I.1. Inhibition parameters of synthesized compounds on the activity of eeAChE

	eeAChE	
Inhibitor	**K_i (µM)**	**IC_{50} (µM)**
Donepezil	0.031 ± 0.022	0.029 ± 0.005
DEMG3	4.400 ± 1.350	2.825 ± 0.625
DEMG5	1.537 ± 0.248	1.249 ± 0.031
DEMG6	0.327 ± 0.010	0.327 ± 0.018
DEMG7	1.417 ± 0.161	1.977 ± 0.173
GP9	0.212 ± 0.078	0.163 ± 0.058
GP10	0.289 ± 0.035	0.331 ± 0.121
GP11	0.426 ± 0.149	0.420 ± 0.294
GP12	3.680 ± 2.350	0.992 ± 0.131
GP13	1.100 ± 0.360	1.430 ± 0.350
GP15	4.125 ± 3.278	6.610 ± 0.099
GP16	1.912 ± 1.128	3.520 ± 0.022
GP17	1.023 ± 0.386	1.748 ± 1.174
GP18	37.453 ± 21.43	40.353 ± 33.63
GP19	20.12 ± 9.43	11.083 ± 1.595

Table I.2 Inhibition parameters and selectivity of synthesized compounds on the activity of hAChE and BuChE.

	hAChE		Bu ChE		Selectivity*	
Inhibitor	**K_i (µM)**	**IC_{50} (µM)**	**K_i (µM)**	**IC_{50} (µM)**	**From K_i**	**From IC_{50}**
Donepezil	0.010 ± 0.006	0.011 ± 0.008	2.140 ± 1.380	1.270 ± 0.410	214	120
DEMG3	2.822 ± 0.022	1.540 ± 0.090	10.611 ± 4.205	7.350 ± 0.130	4	5
DEMG5	4.224 ± 1.920	1.500 ± 0.23	5.613 ± 1.294	5.800 ± 0.050	1	4
DEMG6	0.355 ± 0.035	0.636 ± 0.209	6.480 ± 2.420	4.760 ± 0.041	18	7
DEMG7	1.980 ± 0.180	2.160 ± 0.760	8.460 ± 3.930	7.590 ± 0.03	4	4
GP9	0.035 ± 0.008	0.058 ± 0.033	2.440 ± 1.290	4.740 ± 0.750	71	81
GP11	0.260 ± 0.036	0.342 ± 0.029	1.140 ± 0.052	2.650 ± 0.617	4	8
GP12	1.835 ± 0.597	1.509 ± 0.510	3.099 ± 2.610	1.140 ± 0.090	2	1
GP10	0.029 ± 0.007	0.043 ± 0.007	3.140 ± 1.800	5.734 ± 0.130	110	132
GP17	0.980 ± 0.220	0.755 ± 0.025	7.254 ± 4.572	15.130 ± 0.025	7	20
GP13	0.554 ± 0.052	0.853 ± 0.052	3.490 ± 2.240	2.170 ± 1.330	6	3
GP15	119.490 ± 61.030	34.500 ± 18.470	3.888 ± 3.110	1.620 ± 0.004	<1	<1
GP16	17.230 ± 6.420	12.155 ± 0.225	2.378 ± 1.730	5.410 ± 0.120	<1	<1
GP19	39.670 ± 12.040	25.195 ± 21.720	4.328 ± 2.969	9.820 ± 0.200	<1	<1
GP18	18.200 ± 7.640	11.135 ± 0.054	6.437 ± 2.633	4.820 ± 0.002	<1	<1

*The selectivity was derived from the ratio K_{iBuChE}/K_{iAChE}.

The data on selectivity reported in the Table I.2 indicated that, among the Donepezil analogues synthesized, **GP9** and **GP10** resulted about two orders of magnitude more selective for AChE than BuChE, therefore approaching the selectiveness displayed by Donepezil.

In order to assess the mode of inhibition, the effect of different concentration of the compounds was tested at various thiolated substrate concentrations, allowing the determination of the K_i. Concerning the effect of Donepezil on cholinesterase activity a representative plot of the above mentioned experiments is reported in Figure I.9. The data were either interpolated in the Michaelis-Menten equation or treated with the Lineweaver-Burk equation giving similar results.

The data indicated that among the inhibitors, **GP17**, **GP18,** and **GP19** acted as mixed inhibitors of hAChE, as Donepezil did; vice versa, the other synthesized compounds showed a non-competitive behaviour of the inhibition (not shown).

Concerning the effect on BuChE, **DEMG6**, **DEMG7**, **GP9**, **GP11**, and **GP12** exhibited a mixed inhibition mechanism, as Donepezil did. The remaining compounds acted as no competitive inhibitors except for **GP16**, which showed a competitive inhibition mechanism on BuChE.

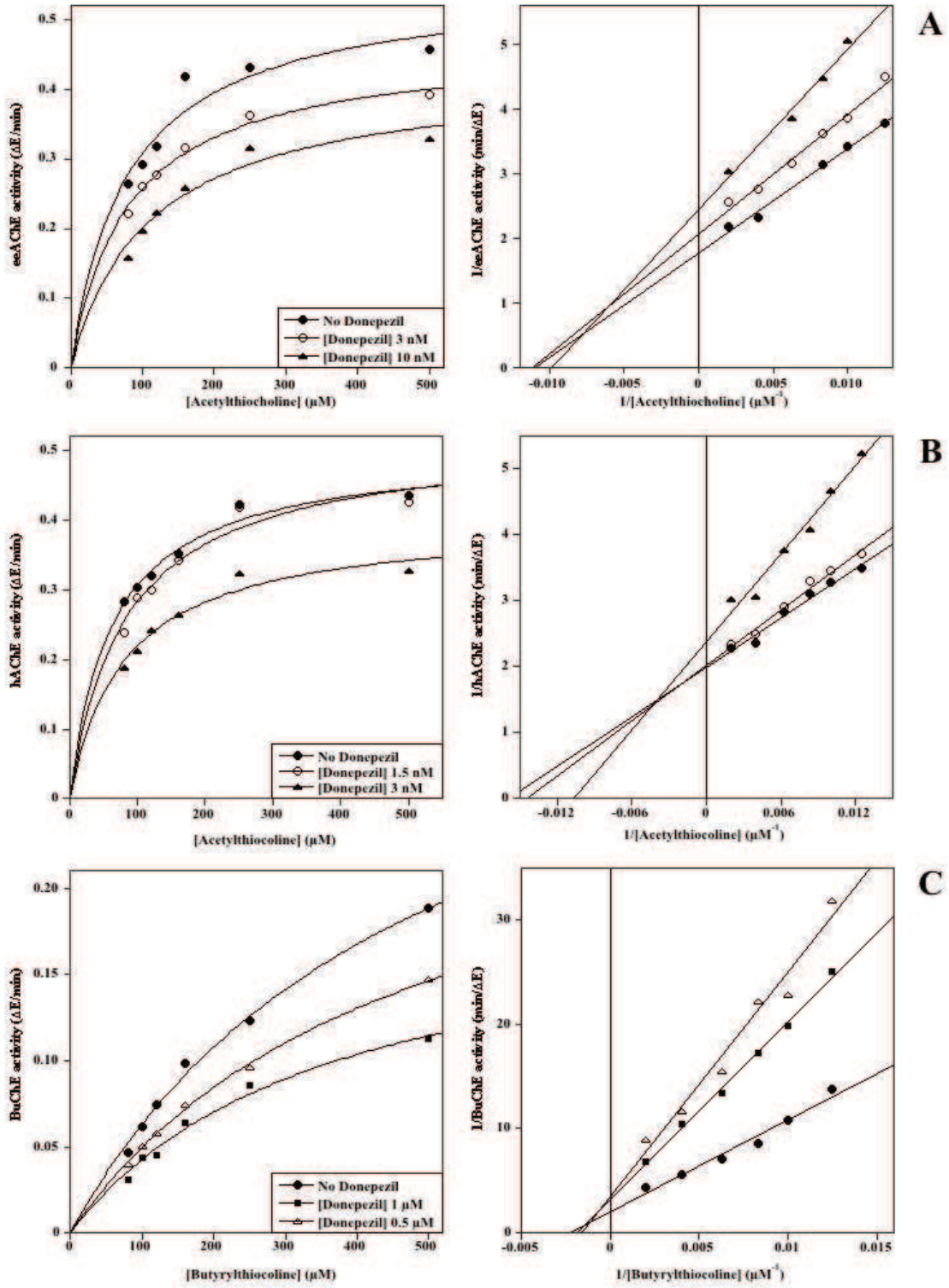

Figure I.9. Determination of the kinetic parameters. The kinetic parameters were determined as reported in the Experimental section I.3.b. Representation of the data with Michaelis-Menten equation (left panels) and Lineweaver-Burk equation (right panels) of Donepezil on eeAChE, hAChE, and BuChE activity (Panel A, B and C, respectively).

I.4.c *Effect of the synthesized compounds on BACE-1 activity*

Using a different experimental approach, the effect of the inhibitors on BACE-1 activity was checked and compared to that exhibited by Donepezil (Fig. I.10). Among the tested compounds **DEMG6**, **DEMG 7**, **GP9**, **GP10**, **GP12** and **GP17**, exhibited the highest inhibition activity, with an estimated IC_{50} below 1 μM, therefore approaching to that shown by Donepezil [Mancini et al., 2007]. Moreover, compared to those reported in the literature for structurally similar molecules, compounds **GP9** and **GP10** displayed a better dual activity and lower IC_{50} values against both AChE and BACE-1 enzymes [Rampa et al., 2015].

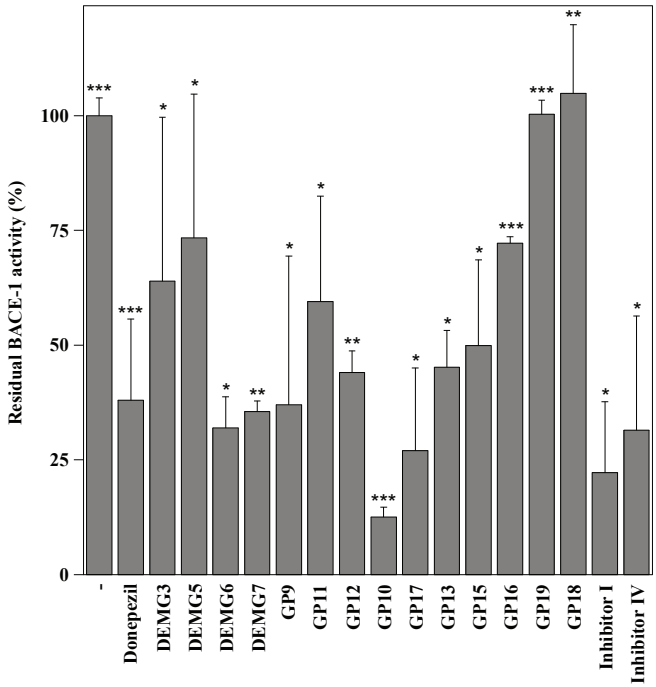

Figure I.10. Effect of synthesized compounds on BACE-1 activity. The BACE-1 activity was determined as reported in the Experimental section I.3.b in the absence or in the presence of 1 μM synthesized compounds. The residual activity was compared to that exhibited by Donepezil (200 nM) or the known Inhibitor I (1 μM) and IV (100 nM) of BACE-1 activity as a positive control. The data represent the average of at least three determinations and the significance of the data was evaluated by *p* value (*, < 0.05; **, < 0.005; ***, < 0.0005).

I.4.d *Effect of the synthesized compounds on proliferation and cell viability of SH-SY5Y neuroblastoma cells*

The effect of the synthesized compounds on proliferation and cell viability was evaluated in SH-SY5Y neuroblastoma cells. In preliminary experiments, the effect of some synthesised compounds (GP9, GP10, GP11, GP12, GP13) was tested adding these molecules at a final concentration ranging from ½– to ten–times their IC_{50} values exhibited towards AChE activity (see Table I.1).

The data showed that none of the inhibitors tested significantly interferes with the proliferation of SH-SY5Y cells up to 48h (Fig. I.11).

Finally, the effect of synthesized compounds on SH-SY5Y cell viability was evaluated using Trypan blue exclusion test. Preliminary results, although not indicating any effect of on cell viability, show that these molecules induce a change in cell morphology (Fig. I.12) passing form a round shaped form to an elongated one.

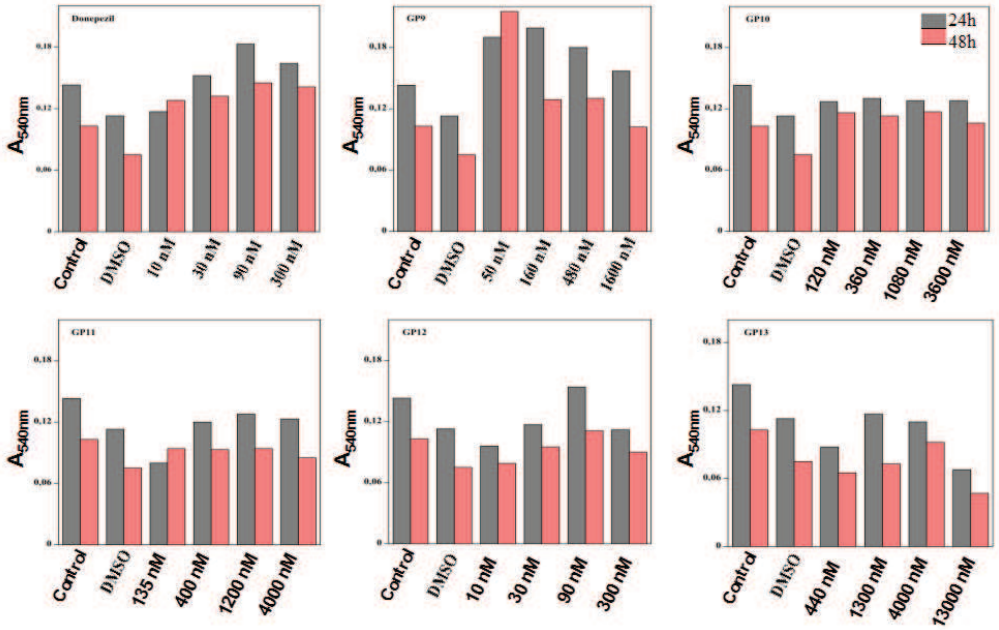

Figure I.11. Effect of synthesized compounds on SH-SY5Y cell proliferation.

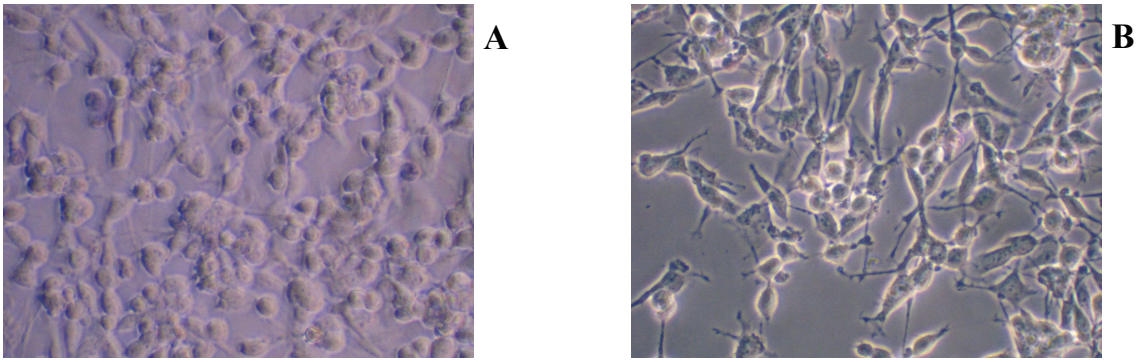

Figure I.12. Effect of synthesized compounds on SH-SY5Y cell viability.

Panel A: control cells; panel B: cells treated with the compound GP10.

Chapter II

Native PAGE to study the interaction between the oncosuppressor p53 and its protein ligands and the dissociation of the complexes by potentially anticancer compounds

II.1 State of art on the methods useful to study the association/ dissociation of p53 complexes

Human p53 is a nuclear phosphoprotein of MW 53 kDa, it was first identified in 1979 by Arnold Levine, David Lane, and Lloyd Old [De Leo et al., 1979]. However its existence was hypothesized first as a target of the oncogenic virus SV40, a strain capable of inducing the development of tumors [Lane & Crawford, 1979; Linzer & Levine, 1979]. Wild-type p53 protein contains 393 amino acids, consisting of three functional domains: an N-terminal activation domain, DNA binding domain, and C-terminal tetramerization domain [Slee et al., 2004; Bode & Dong, 2004; Vousden & Lu, 2002]. The p53 tumor suppressor belongs to a small family of related proteins that includes two other members: p63 and p73. Although structurally and functionally related, p63 and p73 have clear roles in normal development, whereas p53 seems to have evolved in higher organisms to prevent tumour development. In fact, p53 protein is involved in a number of physiological processes [Vousden & Lu, 2002; Vogelstein et al., 2000], and its inactivation/mutation represents one of the most common molecular switch leading to tumorigenesis [Bieging & Attardi, 2012]. As it is involved in roughly one-half of cancers, a great effort has been devoted to the development of strategies targeting the p53 reactivation.

As a tumor suppressor, p53 is essential for preventing inappropriate cell proliferation and maintaining genome integrity following genotoxic stress [Bai & Zhu, 2006]. p53 is activated in response to several malignancy-associated stress signals, resulting in the inhibition of tumour-cell growth. Several responses can be provoked by p53, including cell-cycle arrest, senescence, differentiation and apoptosis,

with the option chosen being dependent on many factors that are both intrinsic and extrinsic to the cell. Under some circumstances, p53 also contributes to the repair of genotoxic damage, potentially allowing for the release of the rehabilitated cell back into the proliferating pool. In most cases, however, induction of p53 leads to an irreversible inhibition of cell growth, most decisively by activating apoptosis [Vousden & Lu, 2002].

Under normal physiological conditions, wild-type p53 protein levels must be kept low owing to its growth-inhibitory activities, and this control is mainly modulated via regulation of p53 protein stability. Although a number of different regulators have been reported to be involved in this protein regulation, MDM2 has been shown to be the principal player in control of p53 turnover [Levine & Oren, 2009].

In fact, probably the most important protein-protein interaction of p53 was discovered, when the MDM2 protein, previously described as a putative oncoprotein, was shown to bind tightly to p53 and inhibit its biochemical activity. MDM2 can inhibit p53 activity by a variety of means. First, by binding to the transactivation domain of p53, hence it sterically blocks the function of that domain. Moreover, by acting as a p53-specific E3 ubiquitin ligase, MDM2 promotes its ubiquitylation and subsequent proteasomal degradation. At the same time, p53 induces the expression of the Mdm2 gene, forming a negative feedback loop [Levine & Oren, 2009].

In 1996, MDM2 was joined by a new homologue, MDMX (MDM4 in the mouse). Like MDM2, MDMX too binds to the N terminal region of p53 and inhibits its activity. While MDMX does not possess measurable E3 activity, it does contribute to p53 degradation; apparently,

dimerization with MDMX augments the E3 ligase activity of MDM2 [Levine & Oren, 2009].

Although a common mechanism involving the binding of the N-terminal hydrophobic domains of MDM2 and/or MDMX to the p53 transactivation domain can be found, several differences can be highlighted between these two inactivators. In addition, a cross-talk between MDM2 and MDMX in targeting p53 is an emerging important finding since it has been implicated in tumorigenesis, therefore, it represents an exciting opportunity in cancer therapy [Wang, 2011; Wang et al., 2012].

Since MDM2 and MDMX play a primary role in inhibition of the p53 tumor suppressor function, blockade of the MDM2/MDMX–p53 protein-protein interaction would liberate p53 from its negative regulators, restoring the tumor suppression function.

The interaction between MDM2/X and p53 has been mapped [Kussie et al., 1996], and on these bases several MDM2/X inhibitors have been designed [Wade et al., 2013], many of which have been submitted to human clinical trials. In fact, almost 10 years later, agents designed to block the MDM2–p53 interaction may have a therapeutic potential application in the discovery of substances with pharmacological activity against cancer development [Vassilev et al., 2004; Wade et al., 2013; Graves et al., 2013; Zhao et al., 2015].

Therefore, a number of techniques have been developed to study the formation and the dissociation of the complexes between these proteins.

Nowadays, the association between the interacting domain of p53 and its protein partners MDM2 and MDMX is studied by different

methods. The same several methodological approaches have been proposed, even to study the dissociation of the p53•MDM2/X complex exerted by molecules with potential pharmacological activity. In particular, nuclear magnetic resonance technology [Daniele et al., 2014], surface plasmon resonance [Vassilev et al., 2004], and fluorescence polarization [Reed et al., 2010] were used to this aim.

Nuclear Magnetic Resonance spectroscopy, most commonly known as NMR spectroscopy is a powerful and theoretically complex analytical tool. This research technique exploits the magnetic properties of certain atomic nuclei. It determines the physical and chemical properties of atoms or the molecules in which they are contained. It relies on the phenomenon of nuclear magnetic resonance and can provide detailed information about the structure, dynamics, reaction state, and chemical environment of molecules. The intramolecular magnetic field around an atom in a molecule changes the resonance frequency, thus giving access to details of the electronic structure of a molecule. Most frequently, NMR spectroscopy is used by chemists and biochemists to investigate the properties of organic molecules, although it is applicable to any kind of sample that contains nuclei possessing spin. NMR spectra are unique, well-resolved, analytically tractable and often highly predictable for small molecules. Thus, in organic chemistry practice, NMR analysis is used to confirm the identity of a substance. A disadvantage is that a relatively large amount, 2–50 mg, of a purified substance is required, although it may be recovered. Preferably, the sample should be dissolved in a solvent, because NMR analysis of solids requires a dedicated MAS machine and may not give equally well-resolved spectra. The timescale of NMR is relatively long, and thus it is

not suitable for observing fast phenomena, producing only an averaged spectrum. Although large amounts of impurities do show on an NMR spectrum, better methods exist for detecting impurities, as NMR is inherently not very sensitive. Finally, NMR spectrometers are expensive.

The ability of the novel compounds to dissociate the MDM2/p53 complex was investigated by NMR and ELISA-based *in vitro* assays on recombinant and native human MDM2/p53 complex, respectively [Daniele et al., 2014].

The inhibition of MDM2-p53 binding was analysed also with Biacore's surface plasmon resonance technology in a solution competition format.

Surface Plasmon Resonance (SPR) is a physical process that can occur when plane-polarized light hits a thin metal film under total internal reflection conditions. The most common use for SPR sensing is to evaluate protein-ligand [Jung et al., 2000], protein-protein [Karlsson & Falt, 1997], or nucleotide hybridization [Moon et al., 2010] events. Since it is typically not advantageous to directly deposit biological molecules onto surfaces, especially surfaces of inert metals such as silver or gold, surface functionalization can be used to create a more functionally active environment and reduce non-specific binding on the surface. Advancements in surface chemistry have allowed researchers to easily customize a sensing surface to their particular needs. In recent years, the information obtained from SPR has also been used to complement the information obtained from mass spectrometry (MS), providing both quantitative and qualitative information. The combined use of SPR and MS can be used for functional proteomic screening,

identifying protein-protein interactions and further characterizing domains involved in the interactions.

Historically, it has been difficult to develop small-molecule inhibitors of non-enzyme protein-protein interactions. However, the crystal structure of MDM2 bound to a peptide from the transactivation domain of p53 [Kussie et al., 1996] has revealed that MDM2 possesses a relatively deep hydrophobic pocket that is filled primarily by three side chains from the helical region of the peptide.

Fluorescence polarization (FP) is a homogeneous method that allows rapid and quantitative analysis of diverse molecular interactions and enzyme activities. This technique has been widely utilized in clinical and biomedical settings, including the diagnosis of certain diseases and monitoring therapeutic drug levels in body fluids. Recent developments in the field has been symbolized by the facile adoption of FP in high-throughput screening (HTS) and small molecule drug discovery of an increasing range of target classes.

Using this approach, it was identified the first MDMX inhibitor, SJ-172550, and demonstrated that it can efficiently kill MDMX-amplified retinoblastoma cells. SJ-172550 functions in an additive manner with the MDM2 inhibitor nutlin-3a, thereby confirming the importance of targeting both of these negative regulators of p53 in cancer cells. This validated MDMX inhibitor provides a valuable lead compound and chemical scaffold for further chemical modification to develop a high affinity MDMX inhibitor with good bioavailability, pharmacokinetics, and pharmacodynamics [Reed et al., 2010].

II.2 The aim

The aim of the present work is to propose a new approach for studying the interaction between p53 and MDM2/X. The method is based on the different mobility between the interacting domains of the oncosuppressor p53 and its protein ligands MDM2/X on polyacrylamide gels under not denaturing conditions.

The novel technique is reliable for determining the different affinity elicited by MDM2 or MDMX toward p53, and can be useful for analysing the dissociation power exerted by other molecules on the p53•MDM2/X complex. It was also investigated if this technique was reliable to determine the dissociative power exerted by small molecules on the complex, when inhibitors are added to the complex mixture. Therefore, it is proposed a new approach to easily screen library of compounds, with potential pharmacological anticancer activity.

II.3 Experimental

II.3.a *Materials*

The protein fragments used in this work were heterologously expressed in *Escherichia coli* using derivatives of the pET-46Ek/LIC vector, in which the nucleotide sequence corresponding to the residues 1–118 of MDM2 (Uniprot accession no. Q00987), 18–102 of MDMX (O15151), and 1–321 of p53 (P04637) was cloned. In the recombinant plasmids, the MAHHHHHHVDDDDK peptide was introduced at the N-terminal of the amino acid sequence of each protein fragment, which allowed the fast purification of the expressed proteins by affinity chromatography. In the case of MDMX, the additional dipeptide IM was inserted at the beginning of the translated amino acid sequence. The plasmids were then used to transform the E. coli BL21 (DE3) RIL strain in which protein expression can be induced by IPTG. Antibodies anti-p53 (A2413 from mouse, monoclonal antibody), anti-MDM2 (LS-C1722 from rabbit, polyclonal), and anti- MDMX (7632 from mouse, monoclonal) were used according to the following dilutions of 1:1000, 1:500,1:500, respectively, and were purchased from Abcam (Massachusetts,US).

Nutlin-3a and Nutlin-3b were from Selleckchem, RO-5963 was from Calbiochem and all the other reagents of electrophoretic and/or molecular biology grade were from Sigma-Aldrich. Stock solutions of the inhibitors were prepared in DMSO at 100 mM final concentration.

II.3.b *Heterologous expression and purification of p53, MDM2 and MDMX protein fragments*

Purified protein fragments were obtained using the procedure previously reported by Daniele et al. [Daniele et al., 2004] with some exceptions. Briefly, bacterial cells from two liters cultures were disrupted by French-Press (Aminco), and the inclusion bodies were prepared by centrifugation at 30 000 × g for 1.5 h. Each pellet was suspended with 5–10 mL of a buffer containing 20 mM Tris–HCl, pH 7.2, 20 mM β-mercaptoethanol, 1 mM PMSF, 1 mM EDTA, and 8 M urea, and centrifuged at 30 000 × g for 1.5 h. The supernatant was incubated with 1 mL of Ni-NTA agarose (Qiagen) over night at 4°C. The slurry was poured into a column, and the packed resin was washed with the above buffer supplemented with 10 mM imidazole. Bound proteins were then eluted with the same buffer in which the concentration of imidazole was raised to 250 mM. Fractions (2 mL) were collected and analysed for purity on 12% w/v SDS-PAGE. The richest and purest fractions (usually the first two or three) were pooled together, diluted (1:5, v/v) with the elution buffer and dialyzed for 2 h at room temperature against the same buffer in which the urea concentration was lowered to 4 M to start renaturation. This was achieved by five dialysis steps at room temperature in which the urea concentration was progressively reduced to 0 M. In the final dialysis step (at 4°C), the buffer was added with 0.5 mM Tris (2-carboxyethyl) phosphine as reducing agent in place of β-mercaptoethanol.

The final protein solutions were concentrated by Centriprep® 10K (Amicon, Germany) up to 1 mg/mL for p53, and 0.5 mg/mL for both MDM2 and MDMX.

The concentrated samples were centrifuged to remove any un-renatured material and stored at 4°C; they were used within 1 month of preparation, before onset of protein precipitation occurred.

Protein concentration was calculated on the basis of the molar extinction coefficient (ε_{280nm}) derived from the amino acid sequence of the three protein fragments using the ProtParam software available at www.swissprot.org. In particular, values of 28420, 10430, and 7450 L mol^{-1} cm^{-1} were calculated for p53, MDM2, and MDMX, respectively.

II.3.c *PAGE under native conditions and densitometric assay*

Electrophoresis was carried out on polyacrylamide gels casted without the stacking gel using the Mini PROTEAN® System of Bio-Rad Laboratories (USA). The separation gel (8 × 7 cm), which was prepared in 375 mM Tris–HCl buffer, pH 8.8, contained 12% w/v acrylamide, 0.3% w/v bisacrylamide, and was polymerized by adding 0.05% v/v TEMED and 0.2% w/v ammonium persulfate. Prior the loading, each sample was incubated for 15 min at 37°C, and added of 8% v/v glycerol; 0.05% w/v bromophenol blue was added to some samples as tracking dye. The electrophoresis run was carried out at 4°C at a constant voltage of 150 V and was stopped after 30 min the tracking dye exited the gel. After the run, protein bands in the gel were fixed and stained with 0.5% w/v CBB-R in 50% v/v methanol and 10% v/v acetic acid and destained with 30% v/v methanol and 7.5% v/v acetic acid.

Gels were dried under vacuum and scanned at 720 dpi. Protein bands were quantified using the ImageJ software (1.43u version) freely available online (http://rsb.info.nih.gov/ij).

II.3.d *Formation of the p53•MDM2/X complex and dissociation by potentially anticancer compounds*

Complex formation was attained by incubating protein fragments at appropriate molar ratios, for 30 min at 37°C.

To check the effect of Nutlin-3a, Nutlin-3b, and RO-5963 as dissociation agents on the p53•MDM2/X complex, they were added to the reaction mixture at a concentration range in line with that used for the same inhibitors, whose effect has been evaluated by other techniques [Vassilev et al., 2004; Daniele et al., 2014]. In particular, in every gel, 11 different concentration of Nutlin-3a (in 40–333 μM range), Nutlin-3b (in 1.3–1667 μM range), or RO-5963 (in 0.104–3.3 μM range), respectively, was added to p53·MDM2 complex. Concerning p53•MDMX complex, the dissociation agents were added to the reaction mixture at different final concentrations; in particular, Nutlin-3b was added in a 133–1667 μM range, Nutlin-3a in a 5–667 μM range, and RO-5963 in a 0.104– 3.3 μM range, respectively, .

The incubation was further prolonged for 15 min at 37°C. At all the concentration used, the effect of the DMSO carried over with the inhibitor concentration was assessed. The mixture of glycerol (8% v/v) and bromophenol blue (0.05% w/v) was added to some samples as tracking dye and then loaded on a 12% polyacrylamide gel (8 × 7 cm, 1-mm thick).

The electrophoresis run and the densitometric quantification of protein bands, was carried out as reported above (Experimental section II.3.c).

II.4 Result and Discussion

II.4.a *Characterization of purified p53, MDM2, and MDMX protein-fragments*

The p53, MDM2, and MDMX protein fragments used in this thesis, corresponded to those involved in the protein-protein interaction. In particular, through molecular biology techniques, a stop codon was inserted after residue 118, 111, and 321 in the nucleotide sequence of the genes encoding MDM2 (Fig. II.1, panel A), MDMX (Fig. II.1, panel B), and p53 (Fig. II.1, panel C). In addition, a peptide spanning 14-15 residues containing six histidine, was inserted at the N-terminus of the fragment, to allow protein purification through affinity chromatography (see Experimental section II.3.b for other details).

The purified protein fragments appeared homogeneous on SDS-PAGE (Fig. II.2), and the calculated molecular mass are in good agreement with those derived from the amino acid sequence.

The identification of purified p53, MDM2, and MDMX protein fragments was obtained by both dot-blotting analysis and MALDI-TOF. In particular, using p53, MDM2, and MDMX antibodies, each purified protein immuno-reacted with its specific antibody, although a slight cross-reaction was found between the p53 antibody and MDM2 protein fragment (Fig. II.3). In addition, MALDI-TOF experiments gave molecular masses and fragmentation patterns expected for all protein fragments (Fig. II.4).

In Table II.1 is reported a comparison between the determined molecular masses of the protein fragments with different methods and those derived from the amino acid sequence. From the analysis of the data

it emerged a discrepancy between the values derived from SDS-PAGE and the other methods for p53 and MDM2. These findings could be related to the fact that these proteins underwent different hydrodynamic behaviour during electrophoresis migration. However, it cannot be excluded that the formation of stable aggregates of p53 or MDM2 impaired SDS denaturation prior the migration.

Panel A

```
                                                                  -11        -1
                                                                MAHH HHHHVDDDDK
        10         20         30         40         50         60         70         80
MCNTNMSVPT DGAVTTSQIP ASEQETLVRP KPLLLKLLKS VGAQKDTYTM KEVLFYLGQY IMTKRLYDEK QQHIVYCSND
        90         100        110        120        130        140        150        160
LLGDLFGVPS FSVKEHRKIY TMIYRNLVVV NQQESSDSGT SVSENRCHLE GGSDQKDLVQ ELQEEKPSSS HLVSRPSTSS
       170         180        190        200        210        220        230        240
RRRAISETEE NSDELSGERQ RKRHKSDSIS LSFDESLALC VIREICCERS SSSESTGTPS NPDLDAGVSE HSGDWLDQDS
       250         260        270        280        290        300        310        320
VSDQFSVEFE VESLDSEDYS LSEEGQELSD EDDEVYQVTV YQAGESDTDS FEEDPEISLA DYWKCTSCNE MNPPLPSHCN
       330         340        350        360        370        380        390        400
RCWALRENWL PEDKGKDKGE ISEKAKLENS TQAEEGFDVP DCKKTIVNDS RESCVEENDD KITQASQSQE SEDYSQPSTS
       410         420        430        440        450        460        470        480
SSIIYSSQED VKEFEREETQ DKEESVESSL PLNAIEPCVI CQGRPKNGCI VHGKTGHLMA CFTCAKKLKK RNKPCPVCRQ
       490
PIQMIVLTYF P
```

Panel B

```
                                                                  -11        -1
                                                              MAHHHH HHVDDDDKIM
        10         20         30         40         50         60         70         80
MTSFSTSAQC STSDSACRIS PGQINQVRPK LPLLKILHAA GAQGEMFTVK EVMHYLGQYI MVKQLYDQQE QHMVYCGGDL
        90         100        110        120        130        140        150        160
LGELLGRQSF SVKDPSPLYD MLRKNLVTLA TATTDAAQTL ALAQDHSMDI PSQDQLKQSA EESSTSRKRT TEDDIPTLPT
       170         180        190        200        210        220        230        240
SEHKCIHSRE DEDLIENLAQ DETSRLDLGF EEWDVAGLPW WFLGNLRSNY TPRSNGSTDL QTNQDVGTAI VSDTTDDLWF
       250         260        270        280        290        300        310        320
LNESVSEQLG VGIKVEAADT EQTSEEVGKV SDKKVIEVGK NDDLEDSKSL SDDTDVEVTS EDEWQCTECK KFNSPSKRYC
       330         340        350        360        370        380        390        400
FRCWALRKDW YSDCSKLTHS LSTSDITAIP EKENEGNDVP DCRRTISAPV VRPKDAYIKK ENSKLFDPCN SVEFLDLAHS
       410         420        430        440        450        460        470        480
SESQETISSM GEQLDNLSEQ RTDTENMEDC QNLLKPCSLC EKRPRDGNII HGRTGHLVTC FHCARRLKKA GASCPICKKE
       490
IQLVIKVFIA
```

Panel C

```
                                                                  -11        -1
                                                                MAHH HHHHVDDDDK
        10         20         30         40         50         60         70         80
MEEPQSDPSV EPPLSQETFS DLWKLLPENN VLSPLPSQAM DDLMLSPDDI EQWFTEDPGP DEAPRMPEAA PPVAPAPAAP
        90         100        110        120        130        140        150        160
TPAAPAPAPS WPLSSSVPSQ KTYQGSYGFR LGFLHSGTAK SVTCTYSPAL NKMFCQLAKT CPVQLWVDST PPPGTRVRAM
       170         180        190        200        210        220        230        240
AIYKQSQHMT EVVRRCPHHE RCSDSDGLAP PQHLIRVEGN LRVEYLDDRN TFRHSVVVPY EPPEVGSDCT TIHYNYMCNS
       250         260        270        280        290        300        310        320
SCMGGMNRRP ILTIITLEDS SGNLLGRNSF EVRVCACPGR DRRTEEENLR KKGEPHHELP PGSTKRALPN NTSSSPQPKK
       330         340        350        360        370        380        390
KPLDGEYFTL QIRGRERFEM FRELNEALEL KDAQAGKEPG GSRAHSSHLK SKKGQSTSRH KKLMFKTEGP DSD
```

Figure II.1. Mapping of the MDM2 (Panel A), MDMX (Panel B) and p53 (Panel C) amino acids regions. Black shadowed residues have been inserted in the expressing plasmids for fast purification of the corresponding proteins. Red shadowed residues are those involved in the interaction between p53 and MDM2 or MDMX.

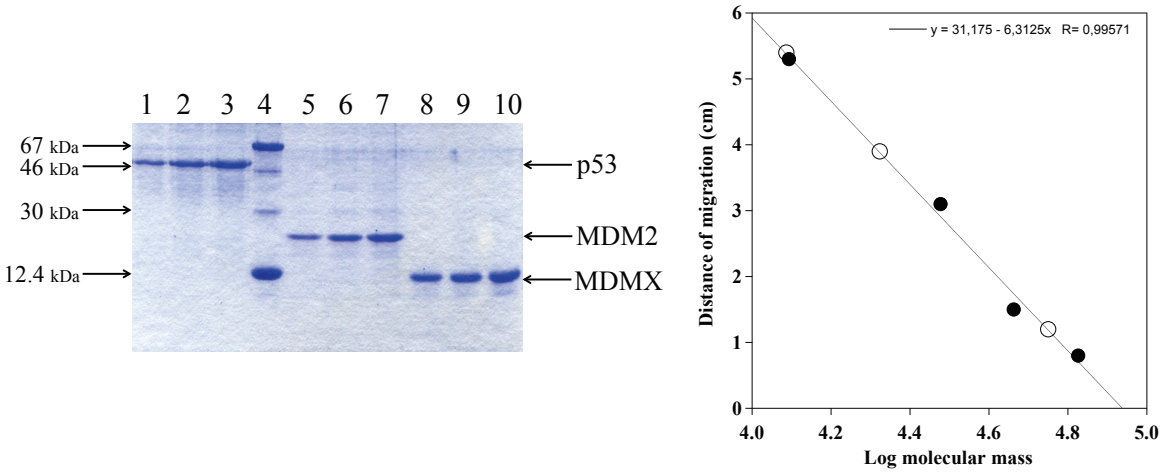

Figure II.2. SDS-PAGE of purified protein fragments and determination of molecular mass.

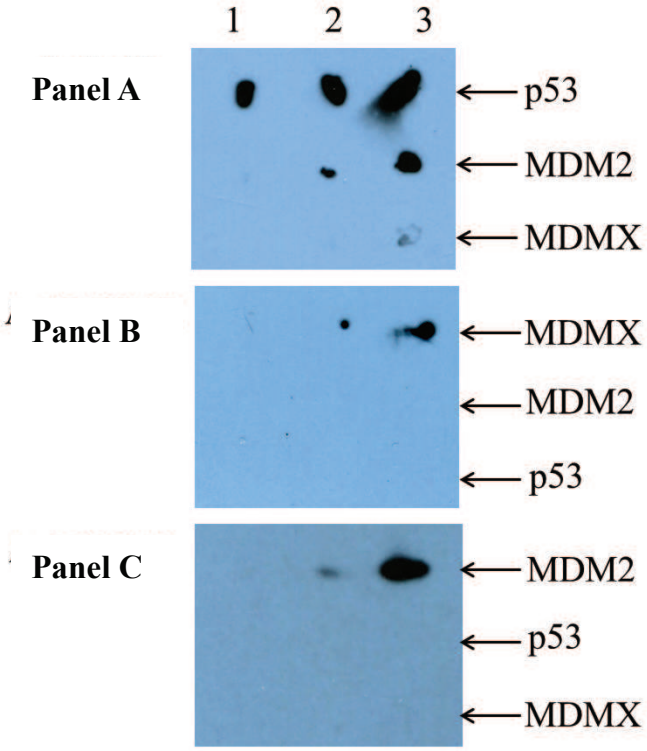

Figure II.3. Identification of purified p53, MDM2, and MDMX protein fragments by dot blotting analysis. 3 ng (lane 1), 30 ng (lane 2) or 300 ng (lane 3) of p53, MDM2 or MDMX were spotted on a nitrocellulose filter previously activated in methanol. After the deposition the filter was incubated with the anti-p53 (A), anti-MDMX (B) or anti-MDM2 (C) antibodies as reported in the 4.II.1 section. Filters were developed according to the chemio-luminescence method using the ECL kit purchased from Millipore.

Panel A

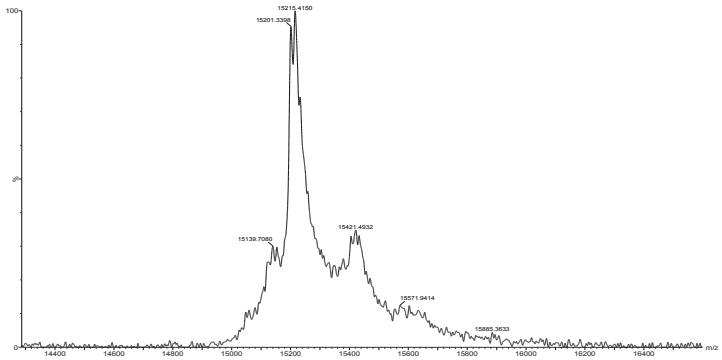

Panel B

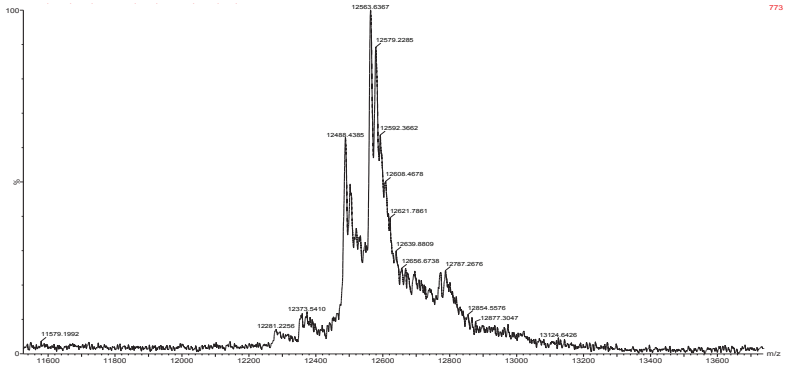

Panel C

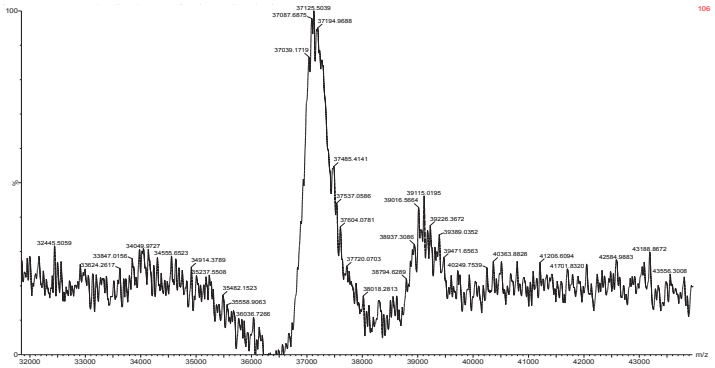

Figure II.4. MALDI-TOF spectra of purified MDM2 (Panel A), MDMX (Panel B) and p53 (Panel C). Mass spectrometry analysis of native proteins was performed with a MALDI–TOF micro MX (Waters Co., Manchester, UK), equipped with a pulsed nitrogen laser (k = 337 nm) as reported. 1µL of the prepared sample was placed on the mass spectrometer and analyzed.
The molecular masses determined for the entire protein fragments expressed (15215, 12564 and 37125 for MDM2, MDMX and p53, respectively) were in good agreement with those derivable from the amino acid sequence of the corresponding protein (15182, 12617 and 37193, respectively).

Table II.1. **Comparison between the molecular mass of p53, MDM2, and MDMX determined with different methods**

	SEQUENCES (Daltons)	SDS-PAGE (Daltons)	MALDI-TOF (Daltons)
p53	37192.8	56260.3	37125.51
MDM2	15182.3	21062.02	15215.41
MDMX	12616.6	12201.13	12563.64

II.4.b *Electrophoresis mobility of p53, MDM2, and MDMX protein interacting fragments on native PAGE*

The interaction between the oncosuppressor p53 and its protein ligands has been studied on native PAGE. Under the experimental conditions reported above (Experimental section II.3.c), p53 did not enter the gel (Fig. II.5A, lane 1), and almost all the loaded protein remained in the well (not shown), a result confirming the property of p53 to form high molecular weight aggregates [Ishimaru et al., 2003]. On the other hand, both MDM2 (Fig. II.5A, lanes 2–5) and MDMX (Fig. II.5A, lanes 10–12) entered the gel and exhibited an electrophoresis mobility that was slightly lower for MDMX. The absence of staining material in the wells excluded the possibility that, under these conditions, insoluble aggregates of these two protein fragments were formed. It is to be pointed out that the stacking gel has to be omitted as MDM2 and MDMX stopped their migration at the interface between the two gels (not shown), a procedure already employed for studying the interaction between elongation factors and some of their interacting molecules [Krasny et al., 1998; Raimo et al.,

2000; Masullo et al., 2000].

A dose-dependent staining was observed for both MDM2 and MDMX, and the plot profile option of the ImageJ (Fig. II.5B) software allowed to derive a relationship between the intensity of the protein bands and their concentration (Fig. II.5, panel C). When p53 and MDM2 or MDMX were mixed together prior loading, a reduction of their signal in the corresponding migrating bands was observed (Fig. II.5A, lanes 6–9 and 13–15 for MDM2 and MDMX, respectively), thus indicating that a stable complex was formed between the two protein fragments. However, under these conditions, at the highest concentration of MDM2 (lane 9) or MDMX (lane 15), the amount of p53 employed was not sufficient to bound all the MDM2/X used. This procedure was then used to study the interaction between p53 and MDM2 or MDMX protein fragments. In fact, as shown in Fig. II.6, the titration of a fixed amount of MDM2 (Fig. II.6A) or MDMX (Fig. II.6B) with increasing amounts of p53 led to the progressive diminution of the intensity of the protein band corresponding to MDM2 or MDMX. The densitometric analysis of protein bands was used for the construction of a dose–effect graph in which a typical saturation behaviour was found (Fig. II.6C). The analysis of the data, according to a hyperbolic equation, confirmed this hypothesis and permitted the extrapolation of the concentration of MDM2/MDMX required to bind half of the amount of p53 used in the assay. The obtained values (2.9 and 9.4 μM for MDM2 and MDMX, respectively), although higher than those determined using a biotinylated p53 peptide in a surface plasmon resonance experiment (0.8 and 2.2 μM, respectively) [Noguchi et al., 2013], confirmed the finding that the affinity for p53 is roughly three-fold higher for MDM2 than that for MDMX.

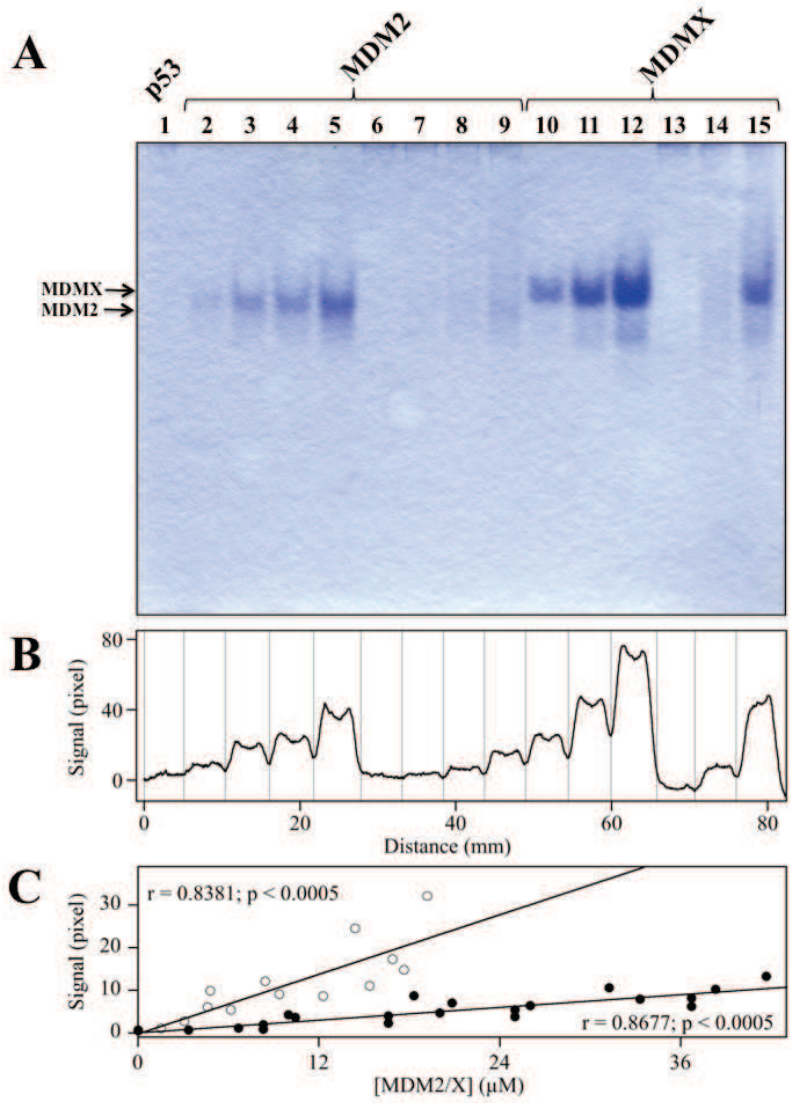

Figure II.5. Electrophoresis mobility of p53, MDM2, and MDMX protein interacting fragments on native PAGE. (A) Migration of p53, MDM2, and MDMX on a 12% w/v native polyacrylamide gel. A 22 μL mixture, prepared as reported in the text (Experimental section 3.II.3), contained 20.4 μM p53 (lane 1); 8.3, 16.6, 25.0, and 36.7 μM MDM2; or 9.2, 18.4, and 33.8 μM MDMX in the absence (lanes 2–5 and 10–12, respectively) or presence (lanes 6–9 and 13–15, respectively) of 20.4 μM p53. The migration of MDM2 and MDMX is indicated with an arrow on the left. (B) Scanning densitometry of the migrating bands reported in (A). (C) Relationship between MDM2/MDMX fragment concentration and intensity signals. The data were derived from three to four different gels run and analysed as in (A) and (B), respectively. The significance of the correlation was evaluated using the statistical parameter *t* in a two-tailed test with 19 and 12 degrees of freedom for MDM2 (filled circles) and MDMX (empty circles), respectively.

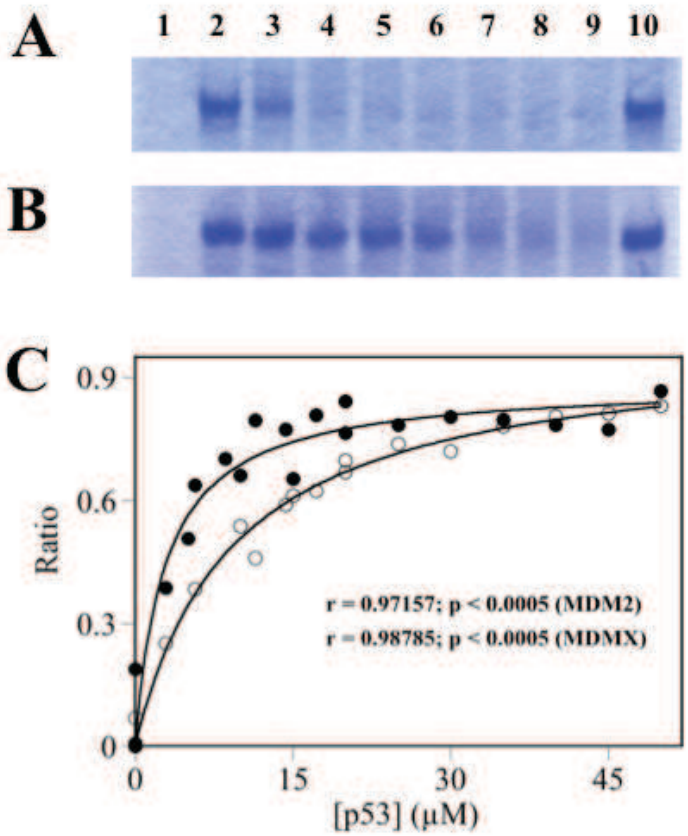

Figure II.6. Titration of MDM2/MDMX with p53. A total of 31.66 μM MDM2 (A) or 14.6 μM MDMX (B) was incubated in the absence (lanes 2 and 10) or presence of 2.9, 5.7, 8.6, 11.4, 14.3, 17.2, and 20 μM p53 (the highest concentration run alone in lane 1) and analysed on a 12% w/v native polyacrylamide gel electrophoresis. The scanning densitometry of the protein band signals on three different gels carried out at different MDM2/MDMX concentration was then derived. The data were reported (C) as the ratio between the amount of unbound MDM2/X (lanes 3–9) and the total con- centration of MDM2/X used (lanes 2 and 10, respectively). Curve fitting was done using the hyperbolic function of the Kaleidagraph software (4.3.1 version). The significance of the correlation was evaluated using the statistical parameter *t* in a two-tailed test with 17 and 13 degrees of freedom for MDM2 (filled circles) and MDMX (empty circles), respectively.

II.4.c *Dissociative effect of Nutlin-3a, Nutlin-3b, andRO-5963 on the preformed p53·MDM2/X complex*

To study the dissociative effect of Nutlin-3a, Nutlin-3b, and RO-5963 on the preformed p53·MDM2 complex, they were added to the reaction mixture. As reported in Fig. II.7, the addition of those inhibitors caused the dissociation of MDM2 from the complex (Fig. II.7A, B, and C, respectively). In addition, the amount of ligand released from the complex increased as the concentration of the dissociation agent increased. The densitometric evaluation of the released MDM2 allowed the determination of the concentration of inhibitor required to dissociate half the complex formed (IC_{50}). In fact, either from the inflection point of a semi-logarithmic plot (Fig. II.7D) or from a saturation behaviour (Fig. II.7E), very similar values of the IC_{50} can be derived and averaged (Table II.2). Although the values obtained are higher than those determined using different methods [Vassilev et al., 2004; Graves et al., 2013], the method confirmed that Nutlin-3a showed a dissociative potency similar to RO-5963, but higher than that elicited by Nutlin-3b.

The results shown in Fig. II.8 confirmed that the method is appropriate as well for the analysis of the p53·MDMX complex dissociation exerted by the above-mentioned inhibitors (Fig. II.8A, B and C, corresponding to Nutlin-3a, Nutlin-3b, and RO-5963 effect, respectively). In fact, either from a semi-logarithmic plot (Fig. II.8E) or from a titration behaviour (Fig. II.8F), the values of the IC_{50} can be derived and are reported in Table II.2. Also in this case, still remaining values of the IC_{50} higher than those reported [Graves et al., 2013], the results confirmed the specificity of RO-5963 toward the dissociation of MDMX from the complex.

An interesting finding emerged when the effect of the inhibitors on the electrophoretic behaviour of the MDM2 or MDMX alone, was considered. In fact, while Nutlin-3a and -3b did not influence the mobility of MDM2 and MDMX (not shown), RO-5963 reduced the mobility of MDMX (Fig. II.8D), but not that of MDM2. In addition, the effect was dose-dependent and, at intermediate concentration, both the fast and slow migrating MDMX bands can be detected in the gel (Fig. II.8D). This finding can be associated with the MDMX oligomerization induced by RO-5963, a behaviour demonstrated using different techniques [Graves et al., 2013]. The effect of RO-5963 on MDMX, was also analysed by gel-filtration, and the results reported in Fig. II.9 confirmed that the inhibitor induced MDMX dimerization. Therefore, the slow $(MDMX)_2$ homodimer migrating rate might indicate a more compact structure of the complex, possessing a lower charge/mass ratio. Also in this case, the densitometric analysis of the gel allowed the determination of the RO-5963 concentration required to half oligomerizate the amount of the MDMX used, either from the fast migrating band disappearing, or from the slow migrating band appearing (Fig. II.8G). Being the obtained value (0.7 μM) identical to that measured for the dissociation of MDMX from a p53·MDMX complex, it can be inferred that the dimerization of MDMX is required to dissociate the complex, thus confirming the results obtained using a different and more complex methodology [Graves et al., 2013].

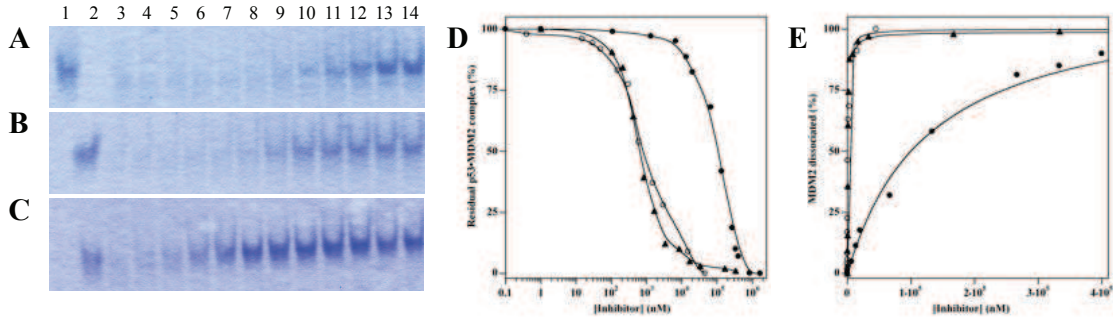

Figure II.7. Dissociative effect of Nutlin3a, Nutlin3b, and RO5963 on the preformed p53·MDM2 complex. Representative electrophoresis polyacrylamide gels in nondenaturing conditions for the analysis of the dissociation power of the inhibitors tested. (A) The reaction mixture containing 25 μM p53·MDM2 complex, treated in the absence (lane 3) or in the presence (lanes 4–14) of 0.040, 0.060, 0.080, 0.12, 0.33, 0.67, 1.33, 3.33, 6.67, 33.33, and 333.33 μM Nutlin-3a, respectively, were run on a 12% nondenaturing polyacrylamide gel. 30 μM MDM2 and p53 was run alone in lanes 1 and 2, respectively. (B) As in (A), but using Nutlin-3b, at concentration of (lanes 4–14) of 1.33, 6.67, 13.33, 20.00, 66.67, 133.33, 266.67, 333.33, 400.00, 833.33, and 1666.67 μM. p53 and MDM2 (25 μM both) were run alone in lanes 1 and 2, respectively. (C) As in (A), but using RO-5963, at concentration of 0.10, 0.21, 0.42, 0.83, 1.67, 3.33, 8.33, 16.67, 33.33, 166.67, and 333.33 μM (lanes 4–14), respectively. (D) The percentage of the residual p53·MDM2 complex was reported in a semilogarithmic plot, at the corresponding concentration of Nutlin-3a (empty circles), RO-5963 (triangles), and Nutlin-3b (filled circles), respectively. (E) The percentage of MDM2 dissociated from the complex was reported as a function of the inhibitor concentration. Curve fitting was done using the hyperbolic function. Symbols as in (D).

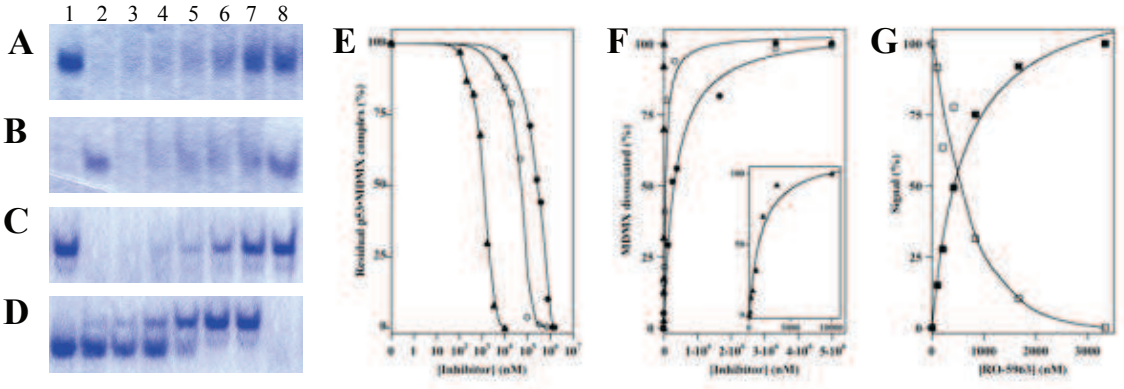

Figure II.8. Dissociative effect of Nutlin-3a, Nutlin-3b, and RO-5963 on the preformed p53·MDMX complex. Representative electrophoresis polyacrylamide gels in nondenaturing conditions for the analysis of the dissociation power of the inhibitors tested. (A) The reaction mixture containing 18 μM p53·MDMX complex treated in the absence (lane 2) or in the presence (lanes 3–8) of 5, 10, 20, 50, 100, 200, 333, and 667 μM Nutlin-3a, respectively, was run on a 12% nondenaturing polyacrylamide gel. Eighteen micromolar MDMX was run alone in lane 1. (B) As in (A), using Nutlin-3b concentration of 0.133, 0.667, 0.400, 1.667, 3.333, and 5 μM Nutlin-3b (lanes 3–8). The migration of the p53·MDMX complex or MDMX alone was analyzed in lanes 1 and 2, respectively. (C) As in (A), using 0.104, 0.208, 0.417, 0.833, 1.667, 3.333, and 10 μM RO-5963 (lanes 3–8). The migration of MDMX alone or in complex with p53 was analyzed in lanes 1 and 2, respectively. (D) The migration of 20 μM MDMX treated in the absence (lane 1) or in the presence of 0.104, 0.208, 0.417, 0.833, 1.667, and 3.333 μM RO-5963 (lanes 1–7) was analyzed. (E) The percentage of the residual p53·MDMX complex, was reported in a semilogarithmic plot, at the corresponding concentration of Nutlin-3a (empty circles), RO-5963 (triangles), and Nutlin-3b (filled circles), respectively. (F) The percentage of MDMX dissociated from the p53·MDMX complex was reported as a function of the inhibitor concentration. Curve fitting was done using the hyperbolic function. Symbols as in (E). (G) The percentage of slow (filled squares) and fast (empty squares) migrating MDMX species (D) were reported as a function of the RO-5963 concentration

Table II.2 Concentration of inhibitors leading to the 50% dissociation of the p53·MDM2/X complex

Inhibitor	Nutlin-3a		Nutlin-3b		RO-5963	
	IC_{50} (μM)	Range (μM)	IC_{50} (μM)	Range (μM)	IC_{50} (μM)	Range (μM)
MDM2	1.8 ± 0.8 (8)	0.04 - 333	99.1 ± 32.9 (8)	1.3 - 1667	0.7 ± 0.1 (4)	0.1 - 3.3
MDMX	67.5 ± 3.9 (4)	5 - 666	270.9 ± 47.0 (4)	133 - 1667	0.7 ± 0.2 (12)	0.1 - 3.3

Values in parentheses indicate the number of gels considered in the analysis. The statistical significance was evaluated in a *t*-Student test; in each cases $p < 0.005$.

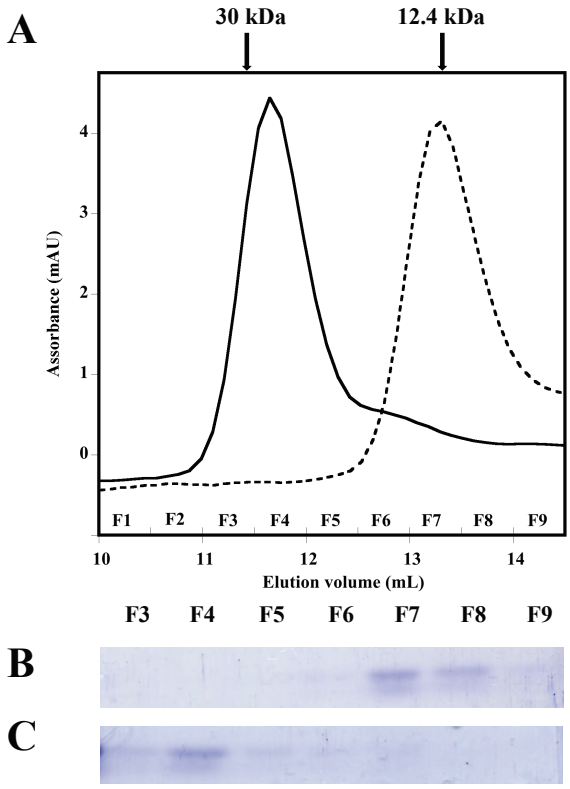

Figure II.9 Analysis on gel-filtration. The effect of RO-5963 on oligomerisation state of MDMX was analyzed by gel-filtration on a Superdex^{TM} 75 10/300 GL column (GE Healthcare) connected to an FPLC^{TM} system. The column was equilibrated at 0.5 mL/min at room temperature (20 – 24°C) with a 20 mM Tris•HCl buffer, pH 7.8, containing 100 mM NaCl, and calibrated with Carbonic Anhydrase (30 kDa), Cytochrome C, (12.4 kDa) (whose elution position was indicated on the top of Panel A), and Ovoalbumin (46 kDa) as protein molecular mass standards. 500–µL fractions were collected, and the protein content was analyzed by 12% SDS-Page. (A) 200–µL (8.4 µM) purified MDMX was analyzed after a 20 min treatment at 37°C in the absence (dashed line), or in the presence of 3.6 µM RO-5963 (continuous line). Both samples eluted as a single peak accounting for molecular masses of 13 kDa and 24 kDa, for the untreated and RO-5963 treated samples, thus confirming that RO-5963 induced MDMX homodimerisation. (B) SDS-Page of the indicated fractions (20 µL) collected from the analysis of the RO-5963 untreated sample. (C) SDS-Page of the indicated fractions (20 µL) collected from the analysis of the RO-5963 treated sample.

Conclusions

The research work carried out in this PhD thesis is focused on the adaptation of common and simple biochemical techniques in order to study the protein-ligand interactions involved in some frequent incidence diseases, such as Alzheimer's disease and cancer. For both topics, a multidisciplinary approach, including pharmacology, bio-informatics, organic chemistry, molecular biology, and of course biochemistry, has been applied.

Although protein-ligand interaction can be studied with a large variety of biophysical techniques, in this thesis two different methodologies were used. From one hand, a molecular enzymology approach allowed the study of the inhibition power exerted by new synthesized donepezil analogues to be used as lead compound for the development of new pharmacological agents for the treatment of Alzheimer's disease. On the other hand, electrophoresis under not denaturing conditions has been used to develop a new analytical method for the characterisation of the interaction between the oncosuppressor p53 and its protein ligands MDM2 and MDMX, as well as the dissociation of the respective complexes.

Regarding the treatment of AD, the enzymatic inhibition tests on AChE and BuChE have been realized on all the synthetized substrate analogues in order to study the influence of the characteristic unsaturation between the two moieties on the Donepezil activity and selectivity. Moreover, a demethylation step was conducted on a set of selected substrates in order to study the role of methoxyl group. All the synthetized derivatives were less active than Donepezil and did not

influenced the cell viability in SH-SY5Y neuroblastoma cells. No improvement in the inhibitor activity was observed with the introduction of hydroxyl groups on the molecules, whereas the substitution of a stereocenter with a double bond, even reducing the inhibition activity on AChE compared to Donepezil, open the possibility to exploit such synthetically simplified Donepezil analogues as better inhibitors of BACE-1. Indeed, compounds **GP9** and **GP10,** considering their selectivity for cholinesterase inhibition and their effect on BACE-1 activity, could represent promising candidates for the development of drugs with dual inhibitor activity for AD treatment.

Regarding the study of the association between the interacting domain of p53 and its protein partners MDM2 and MDMX, it is important to remind that the activation of p53 tumor suppressor by antagonizing its negative regulators MDM2/X has been considered an attractive strategy for cancer therapy. Great effort has been given in the development of drugs able to dissociate the p53·MDM2/X complex. Under this regard, the polyacrylamide gel under native conditions can be useful to easily discriminate, among library of compounds with pharmacological activity against cancer development, the molecules with a remarkable dissociative potency, preventing the use of expensive and more sophisticated technology, as NMR technology [Daniele et al., 2014; D'Silva et al., 2005], surface plasmon resonance [Noguchi et al., 2013], or fluorescence polarization [Reed et al., 2010; Zhang et al., 2013]. The relevance in applying Native-PAGE resides in the fact that it is much simpler and did not require any tagging/derivatization procedure of the protein fragments employed.

Although both research projects deserve further studies, the results here presented are useful for several purposes. Concerning the donepezil-like compounds, a design of new inhibitors will be considered, in particular with the aim to develop drugs endowed with a dual inhibitory effect, like that one observed for GP9 and GP10 compounds. Finally, concerning the gel-shift technique applied to investigate on p53-MDM2/X complex, we will work for a routinely application of this method to quickly analyze new compounds as potential dissociator agents, making even more inexpensive the first screening of molecular libraries, a necessary approach to identify new pharmaceuticals.

References

Alzheimer's disease International. (2011) World Alzheimer Report. 1.

Anand, P. & Singh, B. (2012) a. Synthesis and evaluation of novel carbamate substituted flavanone derivatives as potent acetylcholinesterase inhibitors and anti-amnestic agents. *Medicinal Chemistry Research*, doi: **10**.1007/s00044-012-0162-3.

Bachurin, S.O. (2003). Medicinal chemistry approaches for the treatment and prevention of Alzheimer's disease. *Medicinal Research Reviews*, **23**, 48–88.

Bai, L. & Zhu, W.G. (2006) p53: Structure, Function and Therapeutic Application. *Journal of Cancer Molecules,* **2 (4)**: 141-153.

Bartolini, M., Bertucci, C., Cavrini, V., Andrisano, V. (2003). beta-Amyloid aggregation induced by human acetylcholinesterase: Inhibition studies. *Biochemical Pharmacology,* **65**, 407–416.

Bieging, K.T. & Attardi, L.D. (2012) Deconstructing p53 transcriptional networks in tumor suppression. *Trends Cell Biol.*, **22**, 97–106.

Bode, A.M. & Dong, Z. (2004) Post-translational modification of p53 in tumorigenesis. Nat Rev Cancer, **4**: 793-805.

Bolognesi, M.L., Andrisano, V., Bartolini, M., Banzi, R., Melchiorre, C. (2002) Propidium-Basedpolyamine ligands as potent inhibitors of Acetylcholinesterase and Acetylcholinesterase-Induced Amyloid-β Aggregation. *J. Med. Chem.*, **48**, 24-27.

Zhang, N. & Casida, J.E. (2005) Novel irreversible Butyrylcholinesterase inhibitors: 2-Chloro-1-(substituted-phenyl) ethylphosphonic acids, *Bioorg. Med. Chem.*, **10,** 1281-1290.

Buccafusco, J.J. & Terry, A.V., Jr. (2000) Multiple central nervous system targets for eliciting beneficial effects on memory and cognition. *J Pharmacol Exp Ther*, **295**, 438–446.

Castro, A. & Martinez, A. (2001) Peripheral and dual binding site acetylcholinesterase inhibitors: Implications in treatment of Alzheimer's disease. *Mini Reviews in Medicinal Chemistry,* **1**, 267–272.

D'Silva, L., Ozdowy, P., Krajewsky, M., Rothweiler, U., Singh, M., Holak, T. A. (2005) Monitoring the effects of antagonists on protein-protein interactions with NMR spectroscopy. *J. Am. Chem. Soc.*, **127**, 13220–13226.

Daniele, S., Taliani, S., Da Pozzo, E., Giacomelli, C., Costa, B., Trincavelli, M.L., Rossi, L., La Pietra, V., Barresi, E., Carotenuto, A., Limatola, A., Lamberti, A., Marinelli, L., Novellino, E., Da Settimo, F., Martini, C. (2014) Apoptosis therapy in cancer: the first single-molecule co-activating p53 and the translocator protein in glioblastoma. *Sci. Rep.*, **4**, 4749.

De Ferrari, G.V., Canales, M.A., Shin, I., Weiner, L.M., Silman, I., Inestrosa, N.C. (2001) A structural motif of acetylcholinesterase that promotes amyloid beta-peptide fibril formation. *Biochemistry*, **40,** 10447–10457.

De Leo, A.B., Jay, G., Appella, E., Dubois, G.C., Law, L.W., Old, L.J. (1979) Detection of a transformation-related antigen in chemically induced sarcomas and other transformed cells of the mouse. *Proc Natl Acad Sci,* **76**: 2420-2424.

Dringenberg, H.C. (2000) Alzheimer's disease: More than a ''cholinergic disorder''—Evidence that cholinergicmonoaminergic interactions contribute to EEG slowing and dementia. *Behav Brain Res*, **115**, 235–249.

Eikelenboom, P., Veerhuis, R., Scheper, W., Rozemuller, A.J., van Gool, W.A., Hoozemans, J.J. (2006) The significance of

neuroinflammation in understanding Alzheimer's disease, *J Neural Transm*, **113,** 1685-1695.

Ellman, G.L., Courtney, K.D., Andres, V., Featherstone R.M. (1961) A new and rapid colorimetric determination of acetylcholinesterase activity. *Biochem. Pharmacol*, **7**, 88-95.

Goedert, M., Jakes, R., Spillantini, M.G., Hasegawa, M., Smith, M. J., Crowther, R.A. (1996) Assembly of microtubuleassociatedprotein tau into Alzheimer-like filaments induced by sulphated glyc osaminoglycans, *Nature*, **383**, 550–553.

Graves, B., Thompson, T., Xia, M., Janson, C., Lukacs, C., Deo, D., Di Lello, P., Fry, D., Garvie, C., Huang, K.S., Gao, L., Tovar, C., Lovey, A., Wanner, J., Vassilev, L. T. (2013) Activation of the p53 pathway by small-molecule-induced MDM2 and MDMX dimerization. *Proc. Natl. Acad. Sci.*, **109**, 11788–11793.

Guida, V., Cantarella, M., Chambery, A., Mezzacapo, M.C., Parente, A., Landi, N., Severino, V., Di Maro, A. (2014) Purification and characterization of novel cationic peroxidases from Asparagus acutifolius L. with biotechnological applications. *Mol. Biotechnol.*, **56**, 738–746.

Ishimaru, D., Andrade, L.R., Teixeira, L. S. P., Quesado, P.A., Maiolino, L.M., Lopez, P.M., Cordeiro, Y., Costa, L.T., Heckl, W.M., Weissmuller, G., Foguel, D., Silva, J.L. (2003) Fibrillar aggregates of the tumor suppressor p53 core domain. *Biochemistry*, **42,** 9022–9027.

Jung, L.S., Nelson, K.E., Stayton, P.S., Campbell, C.T. (2000) Binding and dissociation kinetics of wild-type and mutant streptavidins on

mixed biotin-containing alkylthiolate monolayers. *Langmuir*, **16**, 9421-9432.

Karlsson, R. & Falt, A. (1997) Experimental design for kinetic analysis of protein-protein interactions with surface plasmon resonance biosensors. *J. Immunol. Method.*, **200**, 121-133.

Koellner, G., Kryger, G., Millard, C.B., Silman, I., Sussman, J.L., Steiner, T. (2000) (a) Active-site gorge and buried water molecules in crystal structures of acetylcholinesterase from *Torpedo californica*. *J. Mol. Biol*, **296**, 713-735.

Saxena, A., Fedorko, J.M., Vinayaka, C.R., Medhekar, R., Radić, Z., Taylor, P., Lockridge, O., Doctor, B.P. (2003) Aromatic amino-acid residues at the active and peripheral anionic sites control the binding of E2020 (Aricept®) to cholinesterases. *Eur. J. Biochem*, **270**, 4447-4458.

Krasny, L., Mesters, J.R., Tieleman, L.N., Kraal, B., Fucik, V., Hilchenfeld, R., Jonak, J. (1998) Structure and expression of elongation factor Tu from Bacillus stearothermophilus. *J. Mol. Biol.*, **283**, 371–381.

Kussie, P.H., Gorina, S., Marechal, V., Elenbaas, B., Moreau, J., Levine, A.J., Pavletich, N.P. (1996) Structure of the MDM2 oncoprotein bound to the p53 tumor suppressor transactivation domain. *Science*, **274**, 948–953.

Ladner, C.J. & Lee, J.M. (1998) Pharmacological drug treatment of Alzheimer disease: The cholinergic hypothesis revisited. *Journal of Neuropathology and Experimental Neurology*, **57**, 719–731.

Lane, D.P. & Crawford, L.V. (1979) T antigen is bound to a host protein in SV40-transformed cells. *Nature,* **278**: 261-263.

Lavecchia, A., Di Giovanni, C., Pesapane, A., Montuori, N., Ragno, P., Martucci, N.M., Masullo, M., De Vendittis, E., Novellino, E. (2012) Discovery of new inhibitors of Cdc25B dual specificity phosphatases by structure-based virtual screening. *J. Med. Chem*. **55**, 4142-4158.

Levine, A.J. & Oren, M. (2009) The first 30 years of p53: growing ever more complex. *Nature Reviews Cancer,* **9**: 749–758.

Linzer, D.I. & Levine, A.J. (1979) Characterization of a 54K dalton cellular SV40 tumor antigen present in SV40-transformed cells and uninfected embryonal carcinoma cells. *Cell*, **17**: 43-52.

Mancini, F., Naldi, M., Cavrini, V., Andrisano, V. (2007) Multiwell fluorometric and colorimetric microassays for the evaluation of beta-secretase (BACE-1) inhibitors. *Anal. Bioanal. Chem,* **388**, 1175-11831.

Martorana, A., Esposito, Z., Koch, G. (2010) Beyond the cholinergic hypothesis: do current drugs work in Alzheimer's Disease? *CNS Neurosci. Ther*, **16**, 235-245.

Masullo, M., Arcari, P., de Paola, B., Parmeggiani, A., Bocchini, V. (2000) Psychrophilic elongation factor Tu from the antarctic Moraxella sp. Tac II 25: biochemical characterization and cloning of the encoding gene. *Biochemistry*, **39**, 15531– 15539.

Moon, S., Kim, D.J., Kim, K., Kim, D., Lee, H., Lee, K., Haam, S. (2010) Surface-enhance plasmon resonance detection of nanoparticle-conjugated DNA hybridization. *Appl. Opt.*, **49**, 484-491.

Morrison, B.M., Hof, P.R., Morrison, J.H. (1998) Determinants of neuronal vulnerability in neurodegenerative diseases. *Ann Neurol*, **44**, (3 Suppl 1) S32–S44.

Mossman, T. (1983) Rapid colorimetric assay for cellular growth and survival: application to proliferation and cytotoxicity assays. *J. Immunol. Methods*, **65**, 55-63.

Nguyen, V.T., To, D.C., Tran, M.H., Oh, S.H., Kim, J.A., Ali, M.Y., Woo, M.H., Choi, J.S., Min, B.S. (2015) Isolation of cholinesterase and β-secretase 1 inhibiting compounds from Lycopodiella cernua. *Bioorg Med Chem*., **33**, 3126-3134.

Noguchi, T., Oishi, S., Honda, K., Kondoh, Y., Saito, T., Kubo, T., Kaneda, M., Ohno, H., Osada, H., Fujii, N. (2013) Affinity-based screening of MDM2/MDMX-p53 interaction inhibitors by chemical array: identification of novel peptidic inhibitors. *Bioorg. Med. Chem. Lett.*, **23**, 3802–3805.

Ortega, A., Rincón, Á., Jiménez-Aliaga, K.L., Bermejo-Bescós, P., Martín-Aragón, S., Molina, M.T., Csákÿ, AG. (2011) Synthesis and evaluation of arylquinones as BACE1 inhibitors, β-amyloid peptide aggregation inhibitors, and destabilizers of preformed β-amyloid fibrils. *Bioorg Med Chem Lett*, **21**, 2183-2187.

Procopio, A., Alcaro, S., Nardi, M., Oliverio, M., Ortuso, F., Sacchetta, P., Pieragostino, D., Sindona G. (2009) Synthesis, Biological Evalutation, and Molecular Modeling of Oleuropein and Its Semisynthetic Derivatives as Cyclooxygenase Inhibitors. *J. Agric. Food Chem*, **57**, 11161–11167.

Nardi, M., Cozza, A. Maiuolo, L., Oliverio, M., Procopio, A. (2011) 1,5-Benzoheteroazepines through eco-friendly general condensation. *Tetrahedron Lett*., **52**, 4827–483.4.

Cravotto, G., Procopio, A., Oliverio, M., Orio, L., Carnaroglio, D. (2011) Simple sonochemical protocols for fast and repeatable Grignard reactions. *Green Chem*., **13**, 2806–2809;

Oliverio, M., Costanzo, P., Nardi, M., Rivalta, I., Procopio, A. (2014) Facile Ecofriendly Synthesis of Monastrol and Its Structural Isomers via Biginelli Reaction. *ACS Sustainable Chem. Eng.*, **2**, 1228-1233.

Raimo, G., Masullo, M., Lombardo, B., Bocchini V. (2000) The archaeal elongation factor 1alpha bound to GTP forms a ternary complex with eubacterial and eukaryal aminoacyl-tRNA. *Eur. J. Biochem.*, **267**, 6012–6018.

Rampa, A., Mancini, F., De Simone, A., Falchi, F., Belluti, F., Di Martino, R.M., Gobbi, S., Andrisano, V., Tarozzi, A., Bartolini, M., Cavalli, A., Bisi, A. (2015) From AChE to BACE1 inhibitors: The role of the amine on the indanone scaffold. *Bioorg Med Chem Lett.*, **25**, 2804-2808.

Reed, D., Shen, Y., Shelat, A.A., Arnold, L.A., Ferreira, A.M., Zhu, F., Mills, N., Smithson, D. C., Regni, C.A., Bashford, D., Cicero, S.A., Shulman, B.A., Jochemsen, A.G., Guy, R. K., Dyer, M.A. (2010) Identification and characterization of the first small molecule inhibitor of MDMX. *J. Biol. Chem.*, **285**, 10786–10796.

Rees, T., Hammond, P.I., Soreq, H., Younkin, S., Brimijoin, S. (2003) Acetylcholinesterase promotes beta-amyloid plaques in cerebral cortex. *Neurobiology of Aging,* **24**, 777–787.

Selkoe, DJ. (1991) The molecular pathology of Alzheimer's disease. *Neuron*, **6**, 487–498.

Slee, E.A., O'Connor, D.J., Lu, X. (2004) To die or not to die: how does p53 decide? *Oncogene* **23**: 2809-2818.

Sohn, J., Kiburz, B., Li, Z., Deng, L., Safi, A., Pirrung, M.C., Rudolph, J. (2003) Inhibition of Cdc25 phosphatases by indolyldihydroxyquinones. *J. Med. Chem.*, **46**, 2580-2588.

Stachel, S.J., Coburn, C.A., Steele, T.G., Jones, K.G., Loutzenhiser, E.F., Gregro, A.R., Rajapakse, H.A., Lai, M.T., Crouthamel, M.C., Xu, M., Tugusheva, K., Lineberger, J.E., Pietrak, B.L., Espeseth, A.S., Shi, X.P., Chen-Dodson, E., Holloway, M.K., Munshi, S., Simon, A.J., Kuo, L., Vacca, J.P. (2004) Structure-based design of potent and selective cell-permeable inhibitors of human beta-secretase (BACE-1). *J Med Chem.*, **47**, 6447-6450.

Strober, W. (2001) Trypan blue exclusion test of cell viability. *Curr Protoc Immunol,* doi: **10**.1002/0471142735.

Sugimoto, H., Yamanishi, Y., Iimura, Y., Kawakami, Y. (2000) Donepezil Hydrochloride (E2020) and Other Acetylcholinesterase Inhibitors. *Curr. Med. Chem.*, **7**, 303-339.

Van der Zee, E.A., Platt, B., Riedel, G. (2011) Acetylcholine: Future research and perspectives. *Behav. Brain Res.*, **221**, 583-586.

Vassar, R. (2004) BACE-1: the beta-secretase enzyme in Alzheimer's disease. *J. Mol. Neurosci.*, **23**, 105-114.

Vassilev, L.T., Vu, B.T., Graves, B., Carvajal, D., Podlaski, F., Filipovic, Z., Kong, N., Kammlott, U., Lukacs, C., Klein, C., Fotouhi, N., Liu, E.A. (2004) In vivo activation of the p53 pathway by small-molecule antagonists of MDM2. *Science*, **303**, 844–848.

Viayna, E., Sabate, R., Muñoz-Torrero, D. (2013) Dual inhibitors of β-amyloid aggregation andacetylcholinesterase as multi-target anti-Alzheimer drug candidates. *Curr. Top. Med. Chem.*, **13**, 1820-1842.

Vogelstein, B., Lane, D., Levine, A. J. (2000) Surfing the p53 network. *Nature*, **408**, 307–310.

Vousden, K.H. & Lu, X. (2002) Live or let die: the cell's response to p53. *Nature Reviews Cancer*, **2**, 594–604.

Wade, M., Li, Y.C., Wahl, G. M. (2013) MDM2, MDMX and p53 in oncogenesis and cancer therapy. *Nature Reviews Cancer*, **13**, 83–96.

Wang, X. (2011) p53 regulation: teamwork between RING domains of Mdm2 and MdmX. *Cell Cycle*, **10**, 4225–4229.

Wang, X. & Jiang, X. (2012) Mdm2 and MdmX partner to regulate p53. *FEBS Lett.*, **586**, 1390–1396.

Zhang, Q. & Lu, H. (2013) Identification of small molecules affecting p53-MDM2/MDMX interaction by fluorescence polarization. *Methods Mol. Biol.*, **962**, 95–111.

Zhao, Y., Aguilar, A., Bernard, D., Wang, S. (2015) Small-molecule inhibitors of the MDM2-p53 protein-protein interaction (MDM2 Inhibitors) in clinical trials for cancer treatment. *J. Med. Chem.*, **58**, 1038–1052.

Zhu, Y., Xiao, K., Ma, L., Xiong, B., Fu, Y., Yu, H., Wang, W., Wang, X., Hu, D., Peng, H., Li, J., Gong, Q., Chai, Q., Tang, X., Zhang, H., Li, J., Shen, J. (2009) Design, synthesis and biological evaluation of novel dual inhibitors of acetylcholinesterase and beta-secretase. *Bioorg. Med. Chem.*, **17**, 1600-1613.

Ringrazio il Professor Gennaro Raimo, Relatore della Tesi, nonché punto di riferimento per l'intera durata del Dottorato.

Professore *sui generis*, nonostante l'approccio iniziale poco rilassante e abbastanza di impatto, ho avuto la possibilità di conoscere la "persona" e di apprezzarne l'umiltà, il forte senso di giustizia, la maniacale precisione e puntualità, ma anche la sottile ironia e la spiccata personalità partenopea. Lo ringrazio per la professionalità e disponibilità mostratami e per aver fatto di me una persona sicuramente più forte caratterialmente ma anche più precisa e puntuale!

Voglio inoltre rivolgere un ringraziamento speciale al Professor Mario Masullo, una vera e propria guida in questi anni di Dottorato. Non so per quale coincidenza astrale, è apparso durante il mio percorso universitario, dimostrandosi fin dal primo giorno molto disponibile, paziente, gentile e "umano". Nonostante i mille impegni, ha sempre trovato il tempo per indirizzare il mio lavoro di ricerca e di tesi, per consigliarmi e per fornirmi preziosi insegnamenti professionali e non, che spero di aver messo in pratica nel migliore dei modi.

Ringrazio il Professor Paolo Arcari per avermi dato la possibilità di frequentare il laboratorio di Biochimica presso il Dipartimento di Medicina molecolare e Biotecnologie Mediche, dove ho praticamente condotto la maggior parte degli esperimenti del mio lavoro di tesi.

Ringrazio tutti i professori, ricercatori, insomma, tutti gli "abitanti" del VI piano della Torre Biologica; li ringrazio per avermi permesso di lavorare in un clima amichevole, familiare e informale e di essersi sempre dimostrati disponibili a fornirmi utili consigli e chiarimenti per superare i problemi che man mano ho incontrato durante il periodo del dottorato. Tutto questo mi ha permesso di imparare tantissimo e di trarre il meglio da questa esperienza.

Un ringraziamento affettuoso lo rivolgo ai colleghi/amici che hanno reso più spensierate le lunghe giornate, permettondomi così di affrontare il periodo di tesi serenamente, divertendomi molto spesso. Li ringrazio per questa nuova e bella amicizia e gli auguro di poter realizzare tutti i propri progetti, lavorativi e personali.

Un ringraziamento particolare va ad Anna, senza la quale forse questa esperienza non avrebbe mai avuto inizio.

Infine, voglio ringraziare le persone a me più care: i miei genitori, le mie sorelle, i miei nipoti, insomma tutta la mia famiglia che in quest'ultimo periodo mi è stata particolarmente vicino.

Il ringraziamento più grande va a Ciro, la persona che forse più di tutti ha creduto e crede tuttora in me, spesso sopravalutandomi; un vero supporto quotidiano, dalle cui sorprendenti manifestazioni di affetto ho tratto la forza per superare i momenti più difficili e a cui questo lavoro di tesi ho voluto dedicare.